Precambrian Research 370 (2022) 106521

Contents lists available at ScienceDirect

Precambrian Research

journal homepage: www.elsevier.com/locate/precamres

The role of crustal contamination in magma evolution of Neoproterozoic metaigneous rocks from Southwest Svalbard

Karolina Gołuchowska [a,b], Abigail K. Barker [b,*], Maciej Manecki [a,b], Jarosław Majka [a,b], Karolina Kośmińska [a], Robert M. Ellam [c], Jakub Bazarnik [d], Karol Faehnrich [e], Jerzy Czerny [a]

[a] AGH University of Science and Technology, Faculty of Geology, Geophysics and Environmental Protection, al. Mickiewicza 30, 30-059 Kraków, Poland
[b] Mineralogy, Petrology, Tectonics, Department of Earth Sciences, Uppsala University, Villavägen 16, SE-752 36 Uppsala, Sweden
[c] Scottish Universities Environmental Research Centre, East Kilbride G75 0QF, UK
[d] Polish Geological Institute, National Research Institute, Carpathian Branch, Skrzatów 1, 31-560 Kraków, Poland
[e] Department of Earth Sciences, Dartmouth College, Hanover, NH 03755, USA

ARTICLE INFO

Keywords:
Neoproterozoic metavolcanic rocks
Svalbard
Wedel Jarlsberg Land
Nordenskiöld Land
Magma-crust interaction

ABSTRACT

Late Neoproterozoic metavolcanic rocks occur along the Southwest coast of Svalbard. The protoliths of the metavolcanic rocks from Wedel Jarlsberg Land and Nordenskiöld Land are mainly diabase, basalt and felsic tuff of tholeiitic affinity associated with continental magmatism. We investigate the magma evolution of the metavolcanic rocks paying particular attention to processes of magma-crust interaction and assess potential sources of crustal contamination. These goals are achieved by employing trace element geochemistry, as well as Sr and Nd isotope geochemistry. Metavolcanic rocks from the South (Orvindalen and Werenskiöldbreen) have higher LREE, LILE and Th compared to rocks from the North (Nordenskiöld Land), which are relatively enriched in Sr. Incompatible element ratios like Th/La, Th/Nb, La/Nb, Th/Yb and Nb/Yb also decrease from South to North. The $^{143}Nd/^{144}Nd_{(635\ Ma)}$ ranges from 0.511396 to 0.512356 and increases from South to North. For Sr isotopes, the metavolcanic rocks show a wide range, however in the South we observe $^{87}Sr/^{86}Sr_{(635\ Ma)}$ of 0.70407–0.73043 and in the North $^{87}Sr/^{86}Sr_{(635\ Ma)}$ of 0.70410–0.71028. Energy Constrained – Assimilation and Fractional Crystallization (EC-AFC) modelling indicates that the extent of magma contamination is highest in the South. Additionally the modelling suggests fractional crystallization and assimilation of granulite or amphibolite followed by shale for the metavolcanic rocks in the South and for the North mixtures of carbonate and shale contributed. This geographical pattern of assimilation reflects the upper crustal metasedimentary sequences, where phyllites are common in the South (Orvindalen and Werenskiöldbreen) and carbonates are more common in the North (Nordenskiöld Land). Density contrasts and impermeable layers within the continental crust would likely have acted as barriers to ascending magma, forcing it to stall and providing opportunities for magma-crust interaction.

1. Introduction

Volcanism in continental areas requires that magmas generated at depth traverse the continental crust, which provides opportunities for assimilation of crustal materials along the way (e.g. McBirney, 1979; Thompson et al., 1986; Riishuus et al., 2005; Peate et al., 2008; Thorarinsson et al., 2011; Schneider et al., 2016). Geochemical records of magma evolution can be employed to trace the nature of crustal materials interacting with magmas. Additionally, the geochemical records aid our understanding of the crustal compositional structure in a magmatic province as well as potentially providing information on the depth of origin of assimilants, for instance inferences can be drawn from the contribution of lower crustal materials (Dickin, 1994; Peate et al., 2008).

The Precambrian continental crust on Svalbard mostly consists of metasedimentary rocks, such as phyllites, quartzites, schists and metacarbonates together with minor igneous rocks (Figs. 1 and 2; Hjelle et al., 1986; Bjørnerud, 1990; Dallmann et al., 1990; Czerny et al., 1993; Harland, 1997; Dallmann et al. 2015; Majka & Kośmińska, 2017). In addition, amphibolites and orthogneisses occur at deeper tectonostratigraphic levels (Fig. 2; Czerny et al., 1993). Peak metamorphism in the area indicates the lower crust extended down to at least 40 km

* Corresponding author.

https://doi.org/10.1016/j.precamres.2021.106521
Received 27 August 2021; Received in revised form 11 December 2021; Accepted 13 December 2021
Available online 20 January 2022

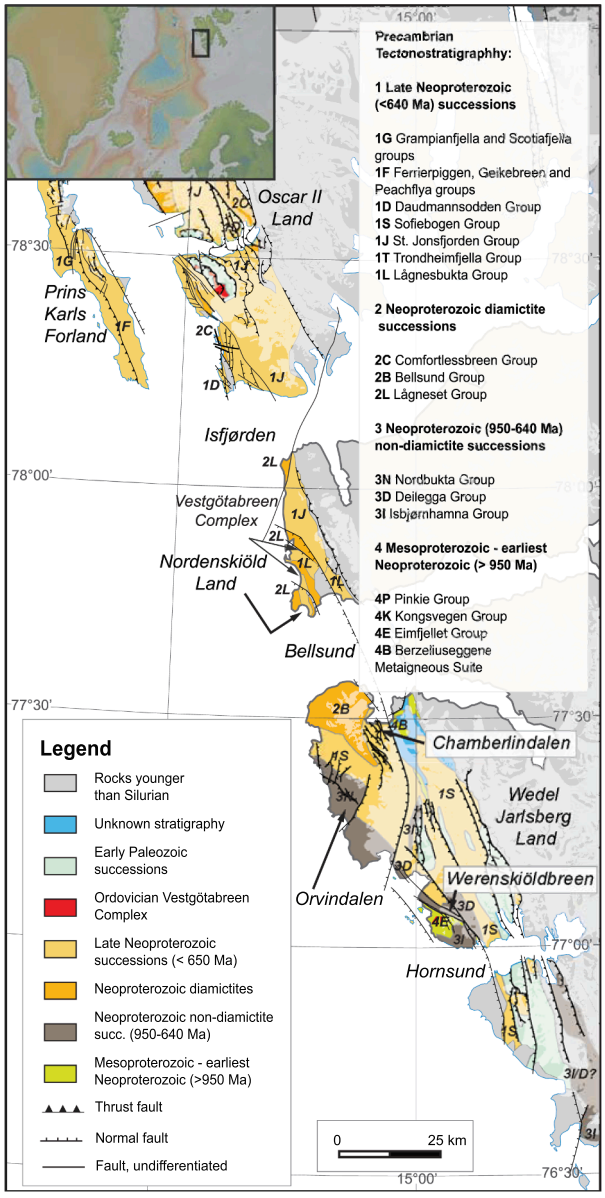

Fig. 1. Geological map of the Southwestern Basement Province with highlighted Precambrian tectonostratigraphy, modified from Dallmann et al. (2015). Samples are retrieved from Nordenskiöld Land, Chamberlindalen, Orvindalen and Werenskiöldbreen, locations are marked with arrows. Inset map shows Svalbard in the context of the Arctic, with Greenland to the West, Iceland to the Southwest and Scandinavia to the South. Inset map courtesy of geomapapp (Ryan et al., 2009).

(Majka et al., 2010, 2015) and is supported by mineral thermobarometry that suggests stagnation and crystallization of magmas at the base of the crust during the Neoproterozoic (Gołuchowska et al., 2016).

The main exposures of metavolcanic rocks interbedded with metasedimentary assemblages in Southwest Svalbard are Neoproterozoic in age, indirectly dated to 635–640 Ma; Wala et al. (2021), and were metamorphosed during the Caledonian orogeny (ca. 450–470 Ma; Gayer et al., 1966; Hjelle et al., 1986; Balashov et al., 1993, 1995, 1996; Harland 1997; Manecki et al., 1998; Gee et al., 2008; Majka et al., 2008, 2012, 2014; Majka & Kośmińska, 2017; Faehnrich et al., 2020). Despite the metamorphic overprint, principal component analysis of trace element compositions of the metavolcanic rocks show geochemical clusters that reflect elemental behavior, indicating preservation of magmatic signatures (Gołuchowska et al., 2012).

This paper focuses on late Neoproterozoic metavolcanic rocks, found in Wedel Jarlsberg Land (Chamberlindalen, Orvindalen and Werenskiöldbreen) and Nordenskiöld Land (Fig. 1), building on the efforts of Ohta (1985), Czerny (1999), and Gołuchowska et al. (2012). New geochemical data for blueschists of the Vestgötabreen Complex from Nordenskiöld Land and Oscar II Land are included for comparison, because they are derived from the same basement province (Kośmińska et al., 2014). We present major and trace element geochemistry along with the first Sr and Nd isotope geochemistry for these rocks to investigate magma evolution, especially magma-crust interaction. The composition of crustal end members is determined by Energy Constrained Assimilation and Fractional Crystallization (EC-AFC) modelling (Bohrson & Spera 2001; Spera & Bohrson, 2001). Furth the distribution of assimilants within the province is integrated with stratigraphic information to provide an holistic perspective of the magmatic system in Southwest Svalbard.

2. Geological background

Ediacaran mafic volcanism is known in the North Atlantic region, mainly from the Baltoscandian margin of Baltica (Ottfjället dike swarm and equivalents; e.g. Gee et al., 2013; Tegner et al., 2019) and it has been dated to ca. 615–590 Ma (e.g. Svenningsen, 2001; Barnes et al., 2019). However, the vast majority of the metavolcanic rocks from Svalbard must have formed during a relatively short time span between 640 and 635 Ma, which makes them substantially older than the Baltoscandian Dike Complex. Hence, the other possible time-equivalent mafic volcanics could be those known from the Pearya Terrane of Ellesmere Island, the latter being anticipated to be a counterpart to western Svalbard (e.g. Gee and Tebenkov, 2004; Mazur et al., 2009; Majka et al., 2021). This volcanic suite has been described in more detail only recently and hypothesized to be connected to Rodinia break-up, but its exact age remains unknown because of limited stratigraphic and geochronological records (Estrada et al., 2018). The only exception in Southwest Svalbard is a gabbro dated to c. 560 Ma and occurs in St. Jonsfjorden area of Oscar II Land (Gumsley et al., 2020). However, this minor lithology clearly cross cuts the major units containing volcanic rocks, whose equivalents are the subject of this study.

The Southwestern Basement Province of Svalbard (SBP) is dominated by weakly metamorphosed Neoproterozoic sedimentary sequences that are juxtaposed with higher grade rocks by the late Caledonian large scale strike-slip shear zones (e.g. Mazur et al., 2009; Majka et al., 2015). These higher grade domains have been recognized along the entire length of the SBP, but only those occurring in Wedel Jarlsberg Land have been characterized in detail (Fig. 1). They are represented by various metaigneous lithologies; metagabbros, metagranitoids and amphibolites of the Eimfjellet Complex that are Ectasian-Stenian in age (1200 Ma; Balashov et al., 1995, 1996), and of the Tonian Berzeliuseggene unit (950 Ma; Majka et al., 2014). In addition Neoproterozoic metasedimentary rocks including metapelites, metapsammites and marbles of the Eimfjellet Complex and Isbjørnhamna Group occur within southern Wedel Jarlsberg Land (Ziemniak et al., 2019). All of these lithologies were metamorphosed under amphibolite facies conditions during the Torellian Orogeny (ca. 640 Ma; Fig. 2; Manecki et al., 1998; Majka et al., 2008, 2010, 2014, 2015).

However, the vast majority of the SBP is comprised of low grade metasedimentary successions. In southern Wedel Jarlsberg Land, the Neoproterozoic Deilegga Group composed of clastic and carbonaceous metasedimentary rocks has been deformed, most probably during the Torellian Orogeny. An erosional unconformity cuts the Deilegga Group, on top of which a series of Marinoan diamictites (i.e. the Slyngfjellet basal conglomerate), dolostones and shales of the Sofiebogen Group have been deposited (Fig. 2; Birkenmajer 1975; Bjørnerud, 1990; Wala et al., 2021). Locally, a thick sequence of glaciomarine conglomerates known as the Kapp Lyell Group covers the Sofiebogen Group. Interestingly, there are mafic dikes cutting through the Deilegga Group rocks

and their geochemical equivalents are found as lavas and tuffs within the overlying Sofiebogen Group (Czerny et al., 1993; Czerny, 1999; Gołuchowska et al., 2012). Hence, it is concluded that these metasedimentary rocks are concurrent with formation of the aforementioned unconformity, whose age is estimated based on deformational, sedimentary, carbon isotope and provenance records to post-640 Ma but pre-Ediacaran (e.g. Ziemniak et al., 2019, Wala et al., 2021). Thus, the emplacement age of subvolcanic intrusions and associated extrusives is bracketed by the Torellian orogenic event at ca. 640 Ma and commencement of sedimentation of the Marinoan Snowball Earth deposits. The latter terminated at 635 Ma (e.g. Condon et al., 2005; Hoffman and Li, 2009) marking *ipso facto* the age limit for the volcanic activity recorded in these strata. The stratigraphic scheme presented above has been adopted in the other parts of Wedel Jarlsberg Land, where there is evidence for an erosional unconformity between the Nordbukta and Dunderbukta/Reserchefjorden groups (Fig. 2; Bjørnerud, 1990). Here, this package of metasedimentary rocks is covered by another thick sequence of the latest Neoproterozoic diamictites of the Kapp Lyell Group. Farther North, in Nordenskiöld Land and Oscar II Land, Neoproterozoic sedimentary sequences containing mafic volcanics are most probably age equivalent to the Sofiebogen Group (Dallmann et al., 2015) and are represented by quartzites, phyllites and metacarbonates (Figs. 1 and 2). Noteworthy, in both Wedel Jarlsberg Land and Nordenskiöld Land, clearly exotic Paleozoic high pressure rocks of the Vestgötabreen Complex are tectonically emplaced onto the Neoproterozoic sequences (e.g. Labrousse et al., 2008, Kośmińska et al., 2014).

The Neoproterozoic metaigneous rocks of the SBP occur within pre-Marinoan and Marinoan metasedimentary rocks along the coast of Wedel Jarlsberg Land and farther North to Nordenskiöld Land and Oscar II Land (Fig. 1; Ohta, 1985; Hjelle et al., 1986; Bjørnerud, 1990; Dallmann et al., 1990; Czerny, 1999; Gołuchowska et al., 2012; Majka & Kośmińska, 2017; Gumsley et al., 2020). The protoliths of the metavolcanic rocks from Werenskiöldbreen in southern Wedel Jarlsberg Land are mainly diabase dikes, basalt lavas and felsic tuffs of tholeiitic affinity associated with within-plate continental magmatism (Czerny, 1999). These metavolcanic rocks occur as greenstones within the Deilegga and Sofiebogen groups and previous literature refers to them as Jens Eriksfjellet metavolcanic rocks (Figs. 2 and 3A; Czerny et al., 1993; Czerny, 1999; Gołuchowska et al., 2012; Majka & Kośmińska, 2017). In central and northern Wedel Jarlsberg Land metatuffs and metabasalts occur e.g. in the Orvindalen, Turrsjødalen and Chamberlindalen valleys within the Sofiebogen Group equivalent metasedimentary rocks (Fig. 3B,C; Bjørnerud, 1990, Dallmann et al., 1990, Wala et al., 2021). Along the western coast of southern and central Nordenskiöld Land massive bodies of metabasites and pillow lavas occur within the late Neoproterozoic metasedimentary rocks (Fig. 3D, E and F). The magmatic province potentially extends further to Oscar II Land, located to the North between Isfjorden and St. Jonsfjorden. On Oscar II Land Ohta et al. (1985) found two kinds of igneous rocks of similar age, metamorphosed under greenschist facies conditions. The first type is metadiabase-gabbro described as moderate to high iron tholeiite, whereas the second is represented mainly by the alkaline Trollheimen volcanics. In comparison to the metaigneous rocks presented here, the

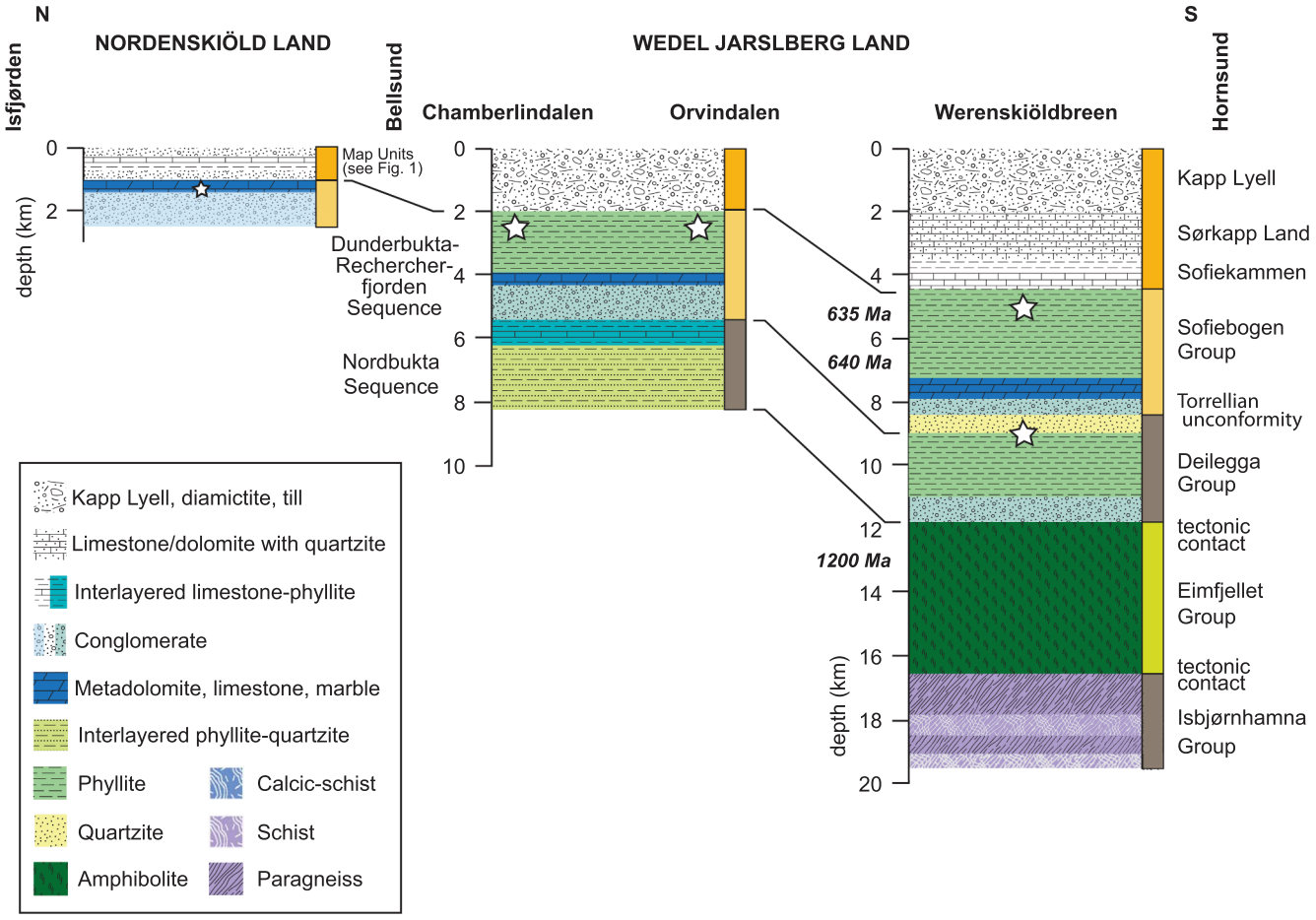

Fig. 2. Lithostratigraphy for Wedel Jarlsberg Land and Nordenskiöld Land based on Hjelle (1962), Birkenmajer (1975), Krasil'shchikov et al. (1979), Hjelle et al. (1986), Bjørnerud (1990), Dallmann et al. (1990) and Czerny et al. (1993). The lithologies of pre-existing and *syn*-volcanic crust are shown in colour, whereas the later sedimentary successions are marked in black and white. Stars mark the approximate appearance of metavolcanics/metaigneous rocks that were sampled for this study.

Fig. 3. Outcrops of metavolcanic rocks on Southwest Svalbard. A) dike cutting metasedimentary rocks of the Deilegga Group in Werenskiöldbreen; B) outcrops of massive metavolcanic rocks in Chamberlindalen; C) metatuffs interlayered with metaconglomerate in Orvindalen; D) uprooted pillow lava from Nordenskiöld Land with *in situ* outcrop of pillow lavas in the background E, F) massive metaigneous rocks from Nordenskiöld Land.

metadiabase-gabbros are the most similar to rocks from Nordenskiöld Land. Also, recent dating of one of such gabbros by Gumsley et al. (2020) clearly shows that they are younger than the major volcanic members of Southwest Svalbard, yet still Neoproterozoic. Hence, they are tentatively correlated with the Seiland Igneous Province of the northern Norwegian Caledonides, but further studies are needed to confirm this link (Ohta, 1985; Majka & Kośmińska, 2017). Also, it should be mentioned here that northern Wedel Jarlsberg Land, Nordenskiöld Land and Oscar II Land were affected by intense deformation during the Eurekan Orogeny (35–65 Ma; e.g. Dallmann et al., 2015; Barnes & Schneider 2019) and locally during the Ellesmerian Orogeny (344–365 Ma; Barnes et al., 2020), which substantially complicates local tectonostratigraphical interpretations.

3. Samples and analytical methods

Metavolcanic rocks from the Svalbard Archipelago have been collected along the southwestern coast of Svalbard during several polar expeditions over several decades. Samples from Werenskiöldbreen (n = 31, Fig. 1), were collected in 1985, 1986 and 1988 (Czerny, 1999). Rocks from Chamberlindalen (n = 2, Fig. 1), were collected during polar expeditions in 2007 and 2008. Samples from Orvindalen (n = 12, Fig. 1), as well as rocks from Nordenskiöld Land (n = 15, Fig. 1), were collected during a polar expedition in 2011. All available samples were analyzed for major and trace elements, and the sample selection for isotope analysis was based on the compositions observed in the major and trace element geochemistry.

Samples from Werenskiöldbreen have previously been analyzed for major elements and Ba, Rb, Sr, Zr, Nb, Y, Ga by X-ray fluorescence (XRF)

at the University of Oslo (Czerny, 1999). Other trace elements were also previously determined by neutron activation analysis and atomic absorption spectroscopy (Czerny, 1999). Additionally, for this study REE, as well as Hf, Ta, Pb, Th and U concentrations for selected samples were determined at the Scottish Universities Environmental Research Centre (SUERC) in East Kilbride, Scotland. At SUERC, powdered whole rocks were dissolved in HNO_3, HF and HCl and then diluted in 200 ml of 5% HNO_3 following the procedure described by Olive et al. (2001) and were analyzed using Inductively Coupled Plasma – Mass Spectrometry (ICP-MS). Calibration was performed with international reference materials and gives uncertainties of 2% RSD (BCR-2 and BCR-1; Olive et al., 2001).

For this study, samples from Orvindalen, Chamberlindalen and Nordenskiöld Land and the blueschists from the Vestgötabreen Complex were crushed and powdered in an agate mortar. Weathered surfaces were removed before crushing and milling. Major and trace element geochemistry was determined by ACME analytical laboratories (Vancouver, Canada). Powders were prepared by lithium borate fusion and analyzed for major elements by Inductively Coupled Plasma – Optical Emission Spectrometry (ICP-OES). For trace elements, samples were prepared using a four acid digestion (HF, HNO_3, HCl, H_2O_2) procedure and analyzed by Inductively Coupled Plasma – Mass Spectrometry (ICP-MS). An internal standard (SO-18; n = 17) records reproducibility of $\leq$ 2% (2 s.d.) for the major elements with the exception of P_2O_5 that has an uncertainty of 4.1% (2 s.d.). For trace elements, three standards have been measured (OREAS24P, OREAS45E, SF-3 T) and typically display reproducibility of 10–20% (2 s.d.). All major and trace element data for all regions are presented in Appendix 1.

Furthermore, for this study 24 samples from Werenskiöldbreen, Orvindalen, Chamberlindalen and Nordenskiöld Land were selected for whole rock Sr and Nd isotope geochemistry. Preliminary Sr and Nd isotopes for three samples from Werenskiöldbreen and two samples from Chamberlindalen were analyzed in the Isotope Geochemistry Laboratory in the Institute of Geological Sciences Polish Academy of Science (IGS PAS) in Kraków. The remaining samples (n = 19) were separated and measured at the Scottish Universities Environmental Research Centre (SUERC) in East Kilbride, Scotland. Whole rock powdered samples were dissolved in HF, HNO_3 and HCl (Anczkiewicz & Thirlwall, 2003, Anczkiewicz et al., 2004; Meyer et al., 2009). Sr and REE were separated by standard cation exchange procedures using AG50Wx8 200–400 mesh cation exchange resin (Anczkiewicz et al., 2004). At the Polish Academy of Sciences, final purification of Sr was conducted with Sr-spec resin (Henderson et al., 1994), whereas Nd was separated by Ln-spec resin (Pin & Zalduegui, 1997; Anczkiewicz & Thirlwall, 2003). Sr and Nd isotope ratios were both measured by Thermal Ionization Mass Spectrometry (TIMS) at SUERC and analyzed by Neptune Multi-Collector Inductively Coupled Plasma Mass Spectrometer (MC-ICP-MS) at IGS PAS. Strontium isotopes were normalized to $^{88}Sr/^{86}Sr = 0.1194$ to correct for mass fractionation (Meyer et al., 2009). The standard (NBS987) analyzed at SUERC gave $^{87}Sr/^{86}Sr$ of 0.710259 ($\pm$0.000018, 2 s.d.), while the standard (NIST SRM987) measured at IGS PAS gave $^{87}Sr/^{86}Sr$ of 0.710261 ($\pm$0.000008, 2 s.d.). Neodymium isotopes were normalized to $^{146}Nd/^{144}Nd = 0.7219$ to correct for instrumental mass bias (Meyer et al., 2009). The standard JNd1Nd measured at SUERC gave $^{143}Nd/^{144}Nd = 0.512116$ ($\pm$0.000022, 2 s.d.) and $^{143}Nd/^{144}Nd = 0.512101$ ($\pm$0.000008, 2 s.d.) at IGS PAS. All standard analyses are close to the long-term values produced by both laboratories (Anczkiewicz et al., 2004; Meyer et al., 2009). Total procedural blanks are all < 300 pg and for Sr at IGS PAS 20 pg. All Sr and Nd isotope data are presented in Appendix 2.

4. Results

4.1. Petrography

The metabasalts from Werenskiöldbreen (n = 31) contain typical greenstone mineral assemblages; albite, actinolite, chlorite and epidote with accessory rutile, titanite, quartz and opaque minerals (Fig. 4A). Relicts of primary plagioclase and clinopyroxene are sericitized and replaced by clinozoisite respectively (Czerny, 1999; Gołuchowska et al., 2012). Aphanitic to porphyritic textures are common, including the occurrence of plagiophyric textures with relicts of primary plagioclase and larger porphyroblasts of secondary plagioclase. Further details can be found in Czerny (1999) and Gołuchowska et al. (2012). The CIPW normative mineral assemblage is plagioclase (61 wt%), hypersthene (10 wt%), diopside (8 wt%) and olivine (3 wt%; Table 1). In addition, the normative assemblage contains minor quartz, orthoclase, nepheline and kalsilite reflecting the metamorphic assemblage and exotic corundum and larnite occur in some samples.

The metavolcanic rocks from Orvindalen (n = 12) are very fine grained to fine grained (Fig. 4B), lineation and foliation are often formed by aligned flakes of muscovite and chlorite. These rocks are classified as mica schist with albite, metamorphosed under low-grade greenschist facies conditions. Field observations indicate that pyroclastic material comprises 20% and 70% of these rocks with the remainder composed of epiclastic material. Hence, the protoliths of these metavolcanic rocks were likely felsic tuff. Primary magmatic minerals and volcanic glass are replaced by Fe and Mg-rich chlorite (20–70% visually estimated by area). Several generations of albite (10–40% visually estimated by area), are observed, one is potentially primary and partly sericitized during metamorphism and the other is fresh and likely secondary albite. Accessory, subhedral to anhedral zircon, apatite and tourmaline with rounded cores overgrown by metamorphic tourmaline are observed. Anhedral and subhedral magnetite crystals are mostly fine grained but larger subhedral and euhedral crystals that usually do not exceed 100 μm also occur (up to ca. 5%). In a few samples, magnetite is overgrown by hematite. Besides magnetite, the opaque minerals are represented by pyrite. The epiclastic material is recrystallized and is represented mainly by quartz (30–70% visually estimated by area) with variable size (from few μm to 100 μm) and flakes of muscovite (10–60% visually estimated by area). Additionally, the epiclastic materials consist of tourmaline and carbonates (up to 10% dolomite and calcite). The CIPW normative mineral assemblage is quartz (36 wt%), plagioclase (24 wt%), orthoclase (22 wt%) and hypersthene (13 wt%), with 1 to 6 wt% corundum (Table 1).

Two samples were collected from Chamberlindalen, one is a metadiabase and the other a greenstone (Fig. 4C, D). The metadiabase has a relict ophitic texture containing large plagioclase (ca. 200 μm and sometimes exceed 1800 μm; 50–70% visually estimated by area) and smaller clinopyroxene crystals (range between ca. 200 μm and 1000 μm; 20–40% visually estimated by area; Fig. 4C). Plagioclase crystals are elongate oligoclase and albite, which show polysynthetic twinning. Polysynthetic twinning was also noticed in some of the clinopyroxene crystals which are often partly altered to chlorite. Additionally, secondary amphibole occurs on the clinopyroxene rims. Interstitially between crystals metamorphic chlorite and rare biotite are found (Fig. 4C). Elongate apatite, titanite and ilmenite pseudomorphs occur as accessory minerals. The greenstone is dominantly composed of remnant plagioclase laths (Fig. 4D). Plagioclase occurs as small albite crystals (ranging from a few μm to ca. 100 μm; 70–80% visually estimated by area) that sometimes show polysynthetic twinning. Chlorite occurs in smaller amounts and usually ranges between a few μm to tens of μm (up to 10% visually estimated by area). Calcite and subhedral titanite occur as accessory minerals. Opaque minerals are common in the Chamberlindalen samples and are composed of pyrite surrounded by goethite. The CIPW normative mineral assemblage contains plagioclase, olivine and pyroxene with secondary orthoclase (Table 1).

The textures of metabasites from Nordenskiöld's Land (n = 15) vary from very fine grained to medium grained and often show foliation formed by alignment of chlorite and sometimes muscovite flakes, as well as actinolite (Fig. 4E, F). In a few samples crenulation cleavage is visible. In outcrops, these metavolcanic rocks are pillow lavas to massive lavas (Fig. 3D, E, F). A few of the pillow lavas have relict amygdaloidal

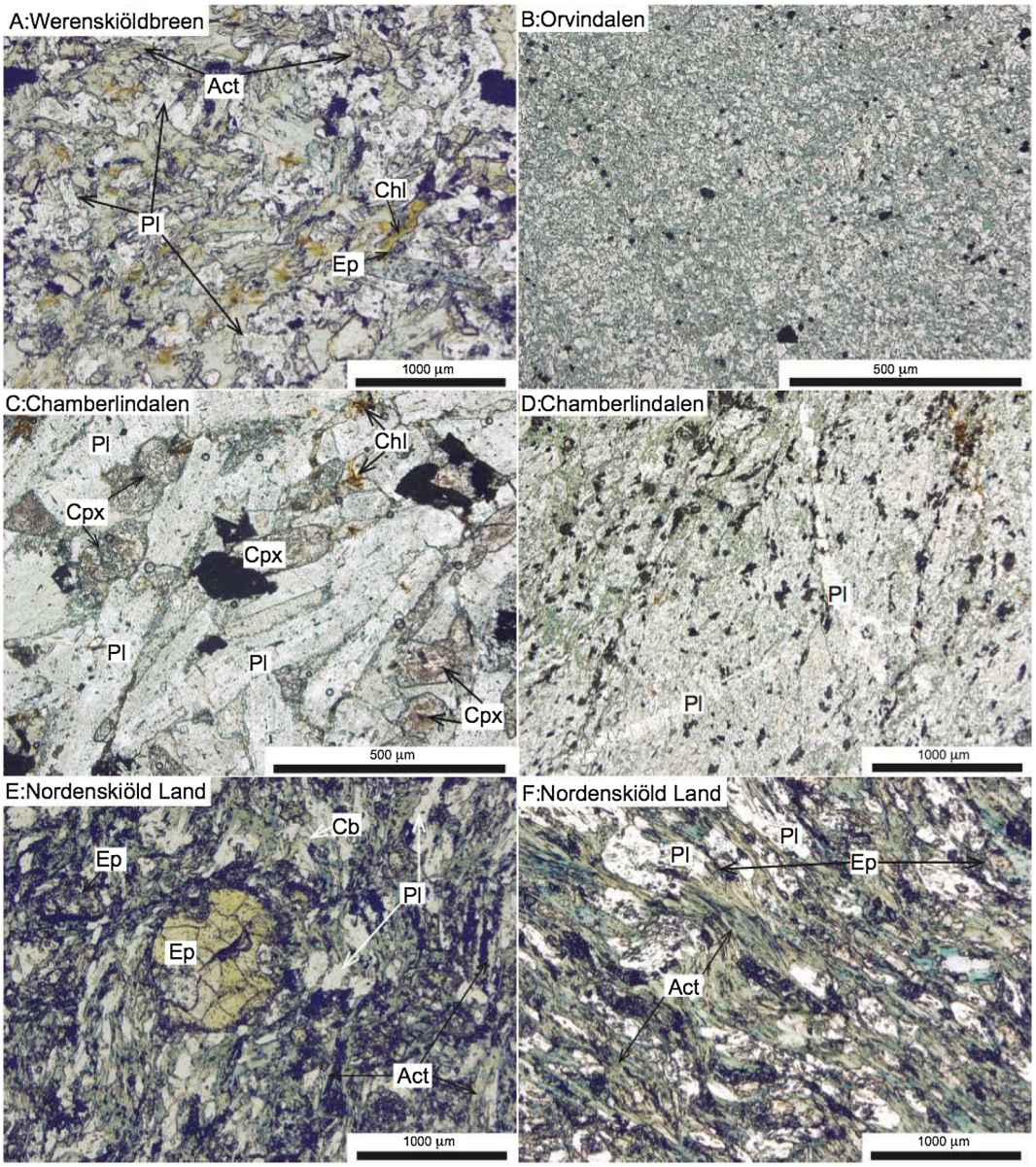

Fig. 4. Photomicrographs of metaigneous rocks of Southwest Svalbard. A) Greenstone from Werenskiöldbreen containing albite, epidote, actinolite and chlorite (PPL), B) fine-grained metatuff collected in Orvindalen that contains quartz, albite and flakes of chlorite (PPL). C) metadiabase from Chamberlindalen, that contains primary plagioclase and pyroxene and metamorphic chlorite (PPL); D) greenstone from Chamberlindalen shows small crystals of albite and chlorite with opaque minerals (PPL); E) metavolcanic rock from Nordenskiöld Land with relict amygdaloidal texture, containing metamorphic albite, actinolite and two generations of epidote: one distributed throughout the sample and a second fills vesicles (PPL); F) greenstone from Nordenskiöld Land with foliation shown by aligned elongated crystals of actinolite (PPL). Abbreviations of mineral names Pl – plagioclase, Cpx – clinopyroxene, Chl – chlorite, Ep - epidote, Act – actinolite and Cb – carbonate.

textures, where the vesicles have been filled by epidote (Fig. 4E). These metavolcanic rocks show different proportions of albite, actinolite, chlorite, epidote, carbonate, quartz and accessory minerals such as titanite, rutile, apatite, garnet and opaque minerals. Mainly anhedral to sometimes subhedral albite and oligoclase are the dominant minerals (20–50% visually estimated by area), which exhibit very variable sizes (from a few µm to >1000 µm), sometimes twinning is observed. Such plagioclase is sometimes observed to break down to sericite. Amphibole is represented mainly by elongate, subhedral to anhedral actinolite (≤30% visually estimated by area) also with sizes ranging from a few µm to 500 µm (Fig. 4E, F). Some of the amphibole shows weak zonation. Euhedral to anhedral epidote (≤40% visually estimated by area), often shows strong zoning and also has a wide range of sizes from a few µm to more than 500 µm (Fig. 4E, F). Additionally, flakes of chlorite are highly abundant in some samples. In a few samples two generations of euhedral and subhedral garnet are observed. A high abundance of garnet occurs in carbonate veins, which sporadically cut the metaigneous rocks. Metamorphic quartz occurs infrequently. Accessory phases include anhedral titanite (up to 5% visually estimated by area) and rare rutile. Opaque minerals are pyrite, goethite and chalcopyrite. The CIPW normative mineral assemblage is plagioclase (60 wt%), diopside (18 wt%), olivine (10 wt%) and hypersthene (8 wt%) with minor secondary orthoclase (<1 wt%; Table 1).

4.2. Geochemistry results

4.2.1. Major and trace elements

Major element geochemistry of rocks from the four regions of Southwest Svalbard reveals overall trends of increasing SiO_2 content with progressively decreasing MgO. The highest MgO contents are

Table 1
CIPW normative mineral assemblages.

	Diopside	Hypersthene	Olivine	Plagioclase	Quartz	Orthoclase	Nepheline	Kalsilite	Corundum	Larnite	Apatite	Iron oxide
Werenskiöldbreen												
24/86C		10.1	3.0	69.9		8.4			1.6		0.4	6.6
115/86A	4.0	19.4		67.2	1.3	4.4					0.5	3.2
113/86A	9.5	10.8	5.2	68.0		1.4					0.5	4.6
68/85A	5.0	11.1	9.9	61.6		6.6					0.7	5.1
14/86A	19.9		8.7	60.4		5.2	1.8				0.5	3.6
164/86C	2.8	4.5	7.6	80.0		1.4					0.4	3.3
148/86C	6.7	9.2	3.7	67.6		10.3					0.4	2.1
21/86A			1.3	2.5			3.2	0.3		91.8	0.1	0.8
164/86A	10.7	17.2		62.2	2.5	1.5					0.7	5.3
109/86A		14.8	7.6	69.8		1.4			0.2		0.7	5.5
156/86B	15.2	7.8		64.8	4.5	1.4					0.4	5.9
3/88A		6.8	5.6	73.6		5.0			3.5		0.4	5.1
23/88A	15.4		0.4	56.2		10.3	12.7				0.5	4.6
126/85	14.3	16.7		60.4	3.8	0.8					0.7	3.3
119/86	8.9	21.8		58.2	2.1						1.5	7.5
118/86A	15.0	13.5		58.6	4.3	0.8					1.2	6.6
Chamberlindalen												
Sp 165/07B	10.7	2.8	12.2	63.9		4.4					0.9	5.2
Sp 168/07A		5.1	8.8	74.7		4.2			1.2		2.2	3.8
Orvindalen												
Sp 01/11		13.6		19.8	30.3	27.9			5.7		0.4	2.3
Sp 02/11		11.0		18.2	38.7	26.3			3.9		0.4	1.5
Sp 03/11		16.8		25.5	32.7	19.1			2.4		0.4	3.1
Sp 04/11		12.1		30.8	39.0	13.6			3.1		0.2	1.2
Sp 05/11		10.6		36.5	33.4	13.6			3.9		0.4	1.5
Sp 06/11		13.5		19.2	39.1	20.6			5.6		0.4	1.6
Sp 07/11		12.0		17.2	35.4	28.1			5.3		0.2	1.8
Sp 08/11		20.8		43.6	20.2	11.0			1.3		0.5	2.9
Sp 09/11		9.6		17.9	40.0	26.3			4.5		0.4	1.4
Sp 10/11		13.6		19.7	40.3	20.1			4.4		0.2	1.7
Sp 11/11		10.7		18.6	36.8	28.3			4.0		0.2	1.4
Sp 12/11		10.6		15.4	41.5	27.7			3.5		0.2	1.1
Nordenskiöld Land												
SP26-11	20.6	1.6	12.4	60.7		1.5					0.2	3.1
SP31-11B	15.5	18.2	2.7	60.5							0.2	2.8
SP32-11C	13.4	7.2	13.7	62.0							0.2	3.5
SP34-11	17.0	7.3	10.6	61.7							0.2	3.3
SP36-11B	21.6	8.5	10.1	56.3							0.2	3.3
SP37-11A	22.7	2.3	9.9	61.3		0.7					0.2	2.8
SP37-11B	14.7	5.2	13.3	62.0		0.7					0.5	3.6
SP38-11	22.6	7.4	7.7	57.4		0.7					0.5	3.8
SP39-11	7.5	11.4	11.6	65.5							0.2	3.8
SP40-11C	21.8	2.9	12.1	55.6		4.4					0.2	2.8
SP42-11	7.6	23.9	3.4	59.6		0.8					0.5	4.3
SP46-11	26.8	8.0	7.3	54.0		0.7					0.2	3.0
SP48-11B	19.3	8.3	5.9	61.0		0.8					0.5	4.2
SP57-11	14.3	5.5	13.9	62.2							0.2	3.9
SP59-11	20.7	7.9	9.1	56.9		0.7					0.5	4.2

recorded in samples from Nordenskiöld Land (5.7–8.3 MgO wt%), followed by Werenskiöldbreen (3.1–8.6 MgO wt%), Chamberlindalen (4.6–5.6 MgO wt%) and Orvindalen (1.9–4.0 MgO wt%) (Fig. 5). The highest SiO_2 contents are found in the metatuffs from Orvindalen (56–68 SiO_2 wt%) with the lowest content of MgO, suggesting that the metatuffs are andesitic to dacitic. This is consistent with the CIPW norm calculations that indicate the compositions of the samples from Nordenskiöld Land, Chamberlindalen and Werenskiöldbreen are plagioclase, pyroxene and olivine normative and can be classified as basalts (Table 1). Whereas the samples from Orvindalen are quartz, plagioclase, orthoclase and hypersthene normative, which highlights their more evolved nature. Generally, with decreasing MgO content, the CaO content also decreases from Nordenskiöld Land samples toward rocks from Orvindalen. Superimposed on the scatter, the TiO_2 and $Fe_2O_3^{(total)}$ content increase slightly, as MgO decreases, until an inflection point at 7 MgO wt %, after which they decrease, with the onset of iron oxide crystallization. The oxides Al_2O_3 and Na_2O also show a slight initial increase and decrease at lower MgO content, reflecting the crystallization of primary plagioclase. Geochemically, the metaigneous rocks from Werenskiöldbreen and usually also Chamberlindalen lie between Nordenskiöld Land and Orvindalen samples. For K_2O, rocks from Orvindalen have the highest content (1.9–4.0 K_2O wt%) and rocks from Nordenskiöld Land show the lowest contents (0.03–0.22 K_2O wt%). For Na_2O rocks from Werenskiöldbreen are elevated and scattered (3.1–5.1 Na_2O wt%), whereas Na_2O contents of rocks from Nordenskiöld Land and Orvindalen have a narrow range at lower concentrations (2.1–3.6 Na_2O wt% and 1.2–3.6 Na_2O wt%, respectively) (Fig. 5). Elevated and scattered values likely reflect the effects of metamorphism on the major element compositions (see Gołuchowska et al., 2012).

The Trollheimen volcanics are similar to the metaigneous rocks from Werenskiöldbreen, however they have higher content of $Fe_2O_3^{(total)}$, TiO_2 and CaO (Fig. 5). Hollocher et al. (2007) investigated dikes from Ottfjället in the Scandian Caledonides, which are slightly younger than our samples and have similar major element contents to rocks in Nordenskiöld Land and some of those from Werenskiöldbreen (Fig. 5). Proximal and coeval blueschists from the Vestgötabreen Complex compare reasonably well with metavolcanic rocks from Nordenskiöld Land and Wedel Jarlsberg Land (Fig. 5; this study; Ohta 1979; Bernard-Griffiths et al., 1993). The blueschists extend to higher contents of MgO, Al_2O_3, and $Fe_2O_3^{(total)}$. However, the blueschists display significantly

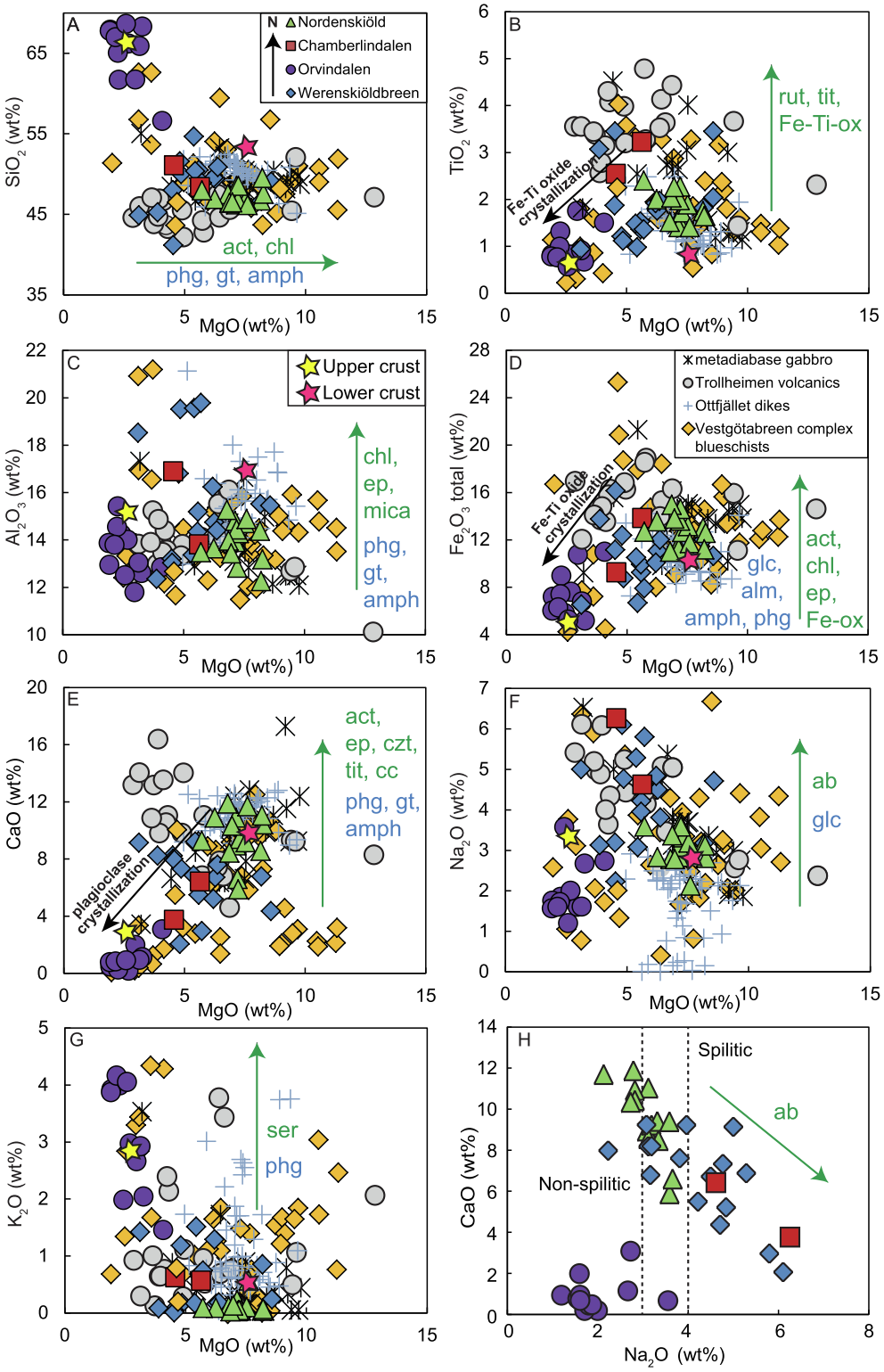

Fig. 5. Whole rock major element geochemistry for metaigneous rocks from Werenskiöldbreen, Orvindalen, Chamberlindalen and Nordenskiöld Land. (A to G) SiO_2, TiO_2, Al_2O_3, Fe_2O_3, CaO, Na_2O and K_2O are shown versus MgO and (H) shows CaO versus Na_2O. For comparison, we also plot greenstones from the adjacent Oscar II Land (metadiabase gabbro and Trollheimen volcanics; Ohta et al., 1985), the Vestgötabreen Complex blueschists from Nordenskiöld land and Oscar II Land (Ohta, 1979; Bernard-Griffiths et al., 1993; this study) as well as Ottfjället dikes from Scandinavia (Hollocher et al., 2007). Upper and lower continental crust have been added for comparison (Rudnick & Gao, 2003). Green arrows indicate metamorphism with greenschist facies minerals denoted in green text and blueschist facies minerals marked by blue text. Abbreviations of minerals are as follows: ab – albite, act – actinolite, alm – almandine garnet, amph – amphibole, cc – calcite, chl – chlorite, czt – clinozoisite, ep – epidote, Fe-Ti-ox - iron titanium oxide, glc – glaucophane, gt –garnet, phg – phengite, rut – rutile, ser – sericite, tit – titanite. (For interpretation of the references to color in this figure legend, the reader is referred to the web version of this article.)

more scatter in CaO, K_2O, TiO_2, and Na_2O than the greenstones (Fig. 5).

Trace element geochemistry for metaigneous rocks from Svalbard reveal elevated and scattered contents of LILE such as Rb, Ba, Sr (Fig. 6A, B, C). Rocks from Nordenskiöld Land have very low contents of Rb and Ba, whereas metatuffs from Orvindalen generally have the highest contents. Metabasalts from Werenskiöldbreen and Chamberlindalen have intermediate trace element concentrations. Besides the scatter in Rb and Ba and the variation with differentiation, it is apparent that the Rb and Ba contents increase and Nb contents decrease in the mafic rocks from the North (Nordenskiöld Land) to the South (Wedel Jarlsberg Land) (Fig. 6A, B and Fig. 7). For Sr, samples from Werenskiöldbreen have a very wide range, the rocks from Nordenskiöld Land and Chamberlindalen show intermediate concentrations of Sr and metaigneous rocks from Orvindalen have the lowest content. It is also worth noticing, that the Sr content of Nordenskiöld Land samples contrasts with the other LILE for this area, they have elevated Sr contents in contrast to the low

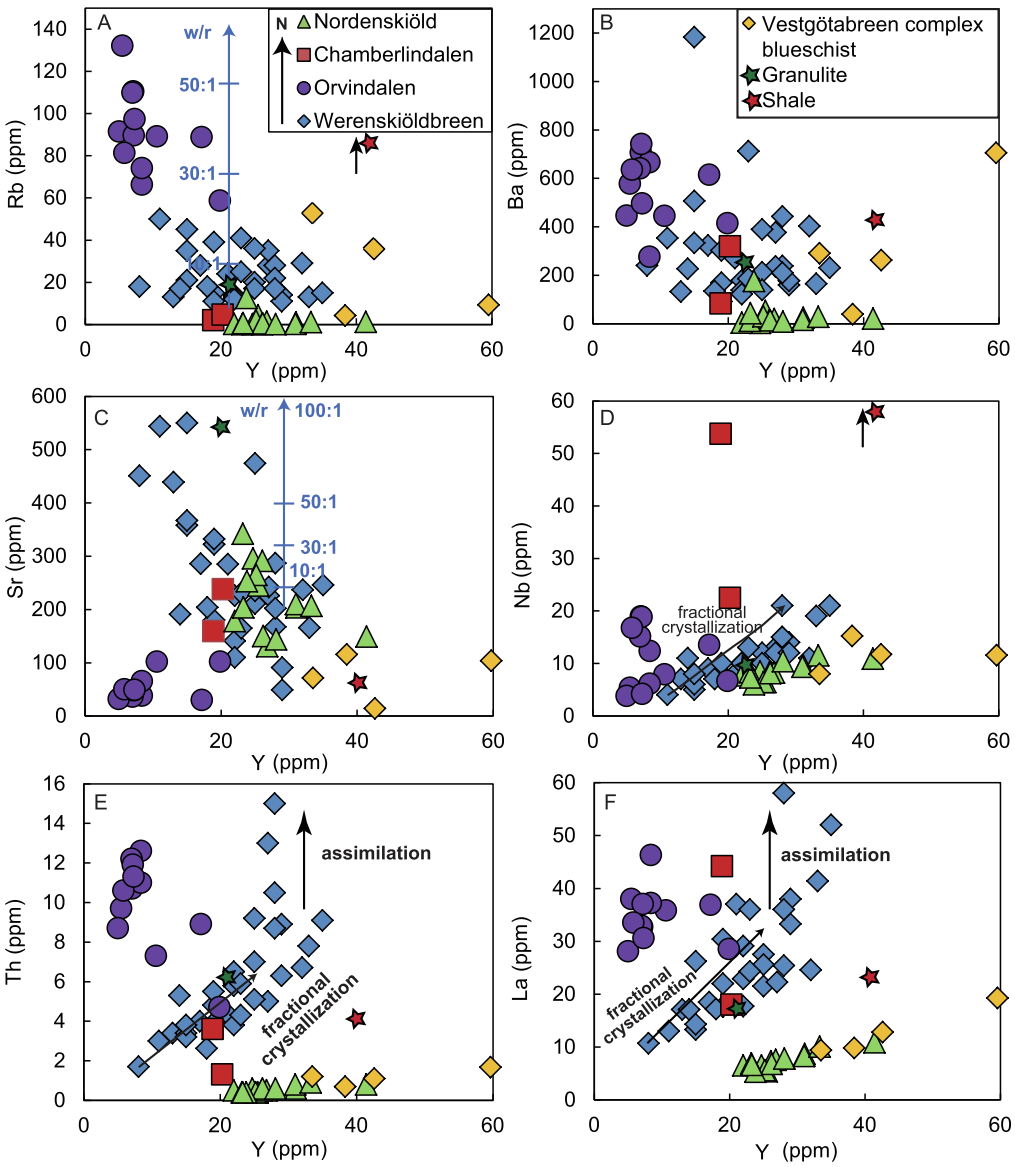

Fig. 6. Trace element geochemistry for metavolcanic rocks from Werenskiöldbreen, Orvindalen, Chamberlindalen and Nordenskiöld Land. (A) Rb, (B) Ba, (C) Sr, (D) Nb, (E) Th and (F) La are plotted versus Y. Fractional crystallization of the Werenskiöldbreen metavolcanic rocks are marked by vectors (See Appendix 3 for model input parameters). The water/rock ratio (w/r) model was based on the Rb and Sr contents of the metavolcanic samples. The fluid composition was derived from fluid/rock partition coefficients of Rb = 2 and Sr = 0.53 (650 °C; Johnson and Plank, 2000) of a Proterozoic metapelite Rb = 21.3 ppm and Sr = 149 ppm (Nelson et al., 1993). The fluid was modelled to precipitate 5% of the trace elements to simulate pervasive alteration due to metamorphism observed in the metavolcanic rocks and outcrops opposed to intense vein networks or fault zones.

Rb and Ba concentrations. Four samples of blueschists from the Vestgötabreen Complex are generally enriched in LILE compared to metaigneous rocks from Nordenskiöld Land and show similar compositions to rocks from Wedel Jarlsberg Land. However they also have low Sr concentrations, which are more similar to metaigneous rocks from Orvindalen (Fig. 6A, B, C).

In terms of Nb, we find distinct compositions for each suite and consequently ΔNb which is neutral for samples from Nordenskiöld Land and slightly negative for samples from Werenskiöldbreen (Fig. 6D, Fig. 7 and Fig. 10D; Fitton et al., 1997). The samples from Orvindalen have unusually positive ΔNb, they generally have lower HFSE content than rocks from the other regions of Southwest Svalbard. The exception is Th, which is high (4.7–12.6 ppm) at Orvindalen in comparison to for example Nordenskiöld Land (<1 ppm; Figs. 6 and 7). Additionally, samples from Nordenskiöld Land also have low HFSE contents and form tight trends. In contrast, the HFSE including REE compositions for samples from Werenskiöldbreen are more scattered, however correlations are apparent between Nb, Th, La and Y. Notwithstanding, some of the samples from Werenskiöldbreen show elevated contents of these immobile elements, especially Th and La (Fig. 6E, F). Generally, the REE for samples from Werenskiöldbreen, Nordenskiöld Land and sometimes rocks from Orvindalen define distinct fractionation trends that are offset from one another as illustrated here for La (Fig. 6F). The four blueschists from the Vestgötabreen Complex are similar to the HFSE differentiation trends for the greenschist metavolcanic rocks from Nordenskiöld Land and extend the trends to higher La, Nb, Th and Y content (Fig. 6D, E, F).

Primitive mantle normalized profiles (Sun & McDonough, 1989) reveal that the metaigneous rocks from Nordenskiöld Land show low LILE and LREE and have generally high Sr concentrations (Fig. 7A). The two samples from Chamberlindalen have the highest Nb and Zr with similar REE to the samples from Orvindalen and Werenskiöldbreen (Fig. 7B). The metavolcanic rocks from Orvindalen and Werenskiöldbreen display the highest Rb, Ba, Th and REE abundances at the lowest Nb contents (Fig. 7C and D). In turn, rocks from Orvindalen have the lowest Sr contents and Werenskiöldbreen samples have the highest Zr concentrations. In comparison to the blueschists from the Vestgötabreen Complex, the metavolcanic samples are generally similarly or more enriched in most trace elements, especially Rb, Ba, Th, U, K and Sr, where the blueschists exhibit low values (Fig. 7). The blueschists often display higher Zr, Ti, Y, Yb and Lu contents than the metavolcanic rocks. The samples from Nordenskiöld Land are distinctive and relatively depleted in trace elements compared to the blueschists especially in Ba and Rb (Fig. 7A).

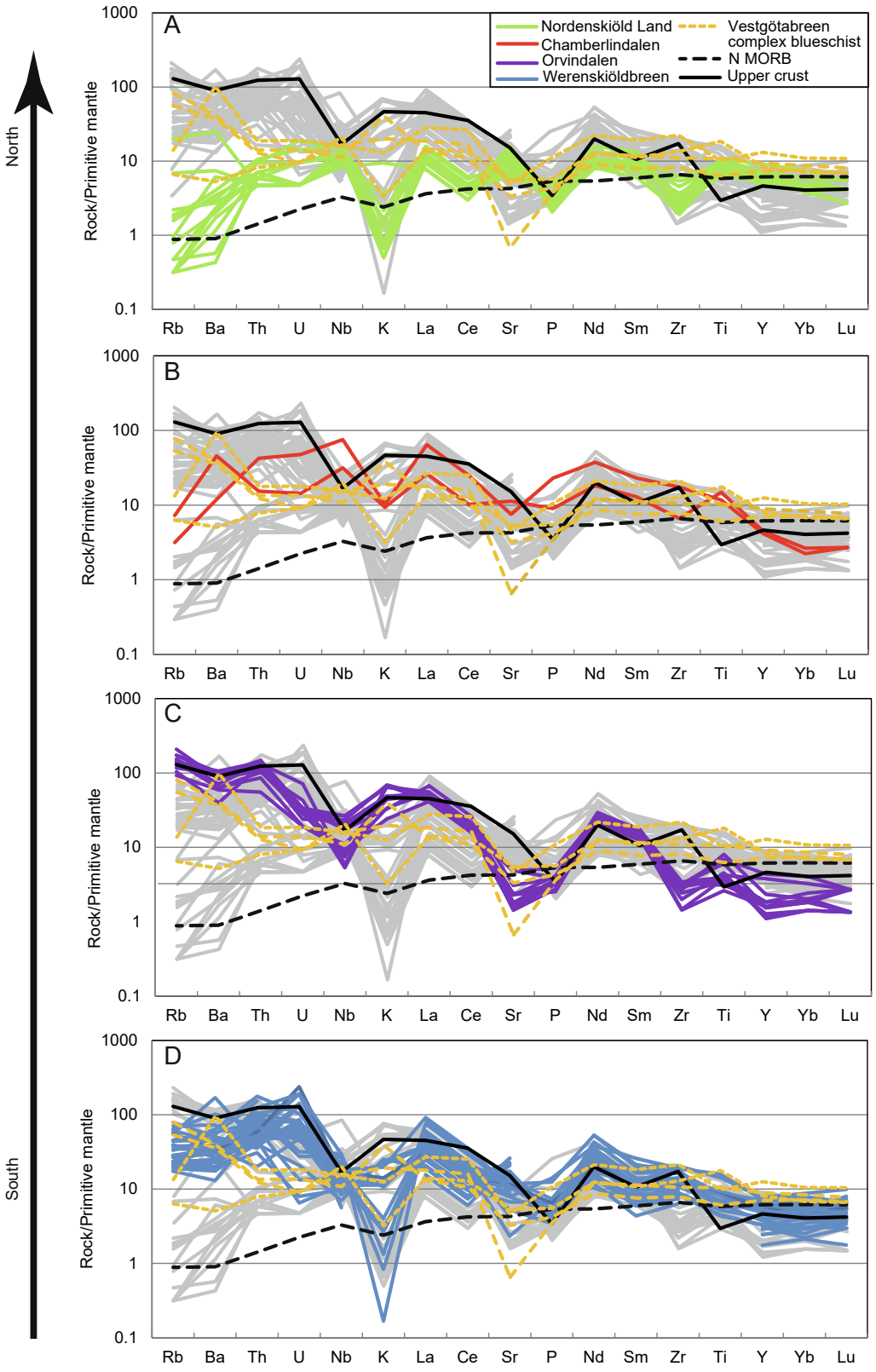

Fig. 7. Spider diagrams normalized to primitive mantle (Sun and McDonough, 1989). In each panel the metavolcanic rocks from the other localities are shown in grey. For comparison average upper crust (Rudnick & Gao, 2003), N-MORB (Sun and McDonough, 1989) and blueschists from Vestgötabreen Complex are presented.

4.2.2. Isotope geochemistry

All samples have been age corrected to 635 Ma with the $^{87}Rb/^{86}Sr$ and $^{147}Sm/^{144}Nd$ ratios displayed in Appendix 2. The samples from Nordenskiöld Land have the highest $^{143}Nd/^{144}Nd_{(635\ Ma)}$ 0.512119–0.512356 ($\varepsilon_{Nd(635\ Ma)}$ +5.8 to +10.3) and extend to relatively high $^{87}Sr/^{86}Sr_{(635\ Ma)}$ of 0.704177–0.710285 (Fig. 8A). In contrast the metatuff samples from Orvindalen, show a wide range of $^{87}Sr/^{86}Sr_{(635\ Ma)}$ 0.715440–0.730429 extending to the highest observed ratios and the

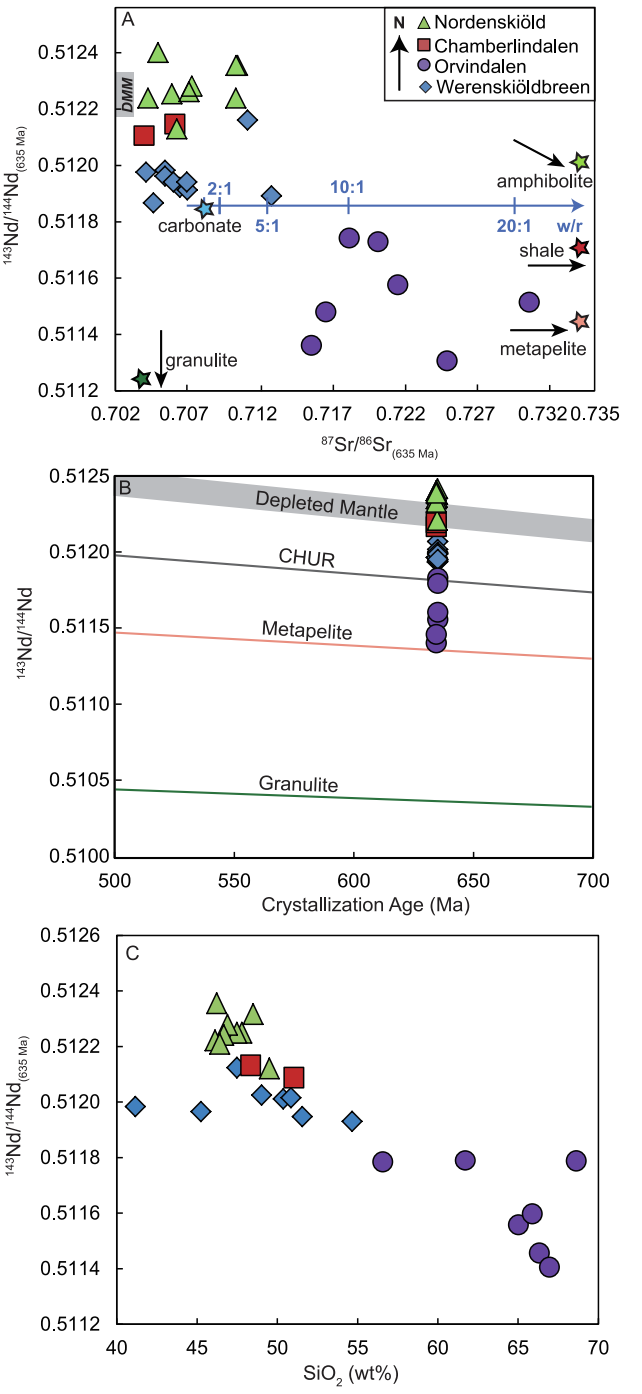

(caption on next column)

Fig. 8. A) Nd and Sr isotope data for the Werenskiöldbreen, Orvindalen, Chamberlindalen and Nordenskiöld Land samples indicate a negative trend in Nd and Sr isotopes for Werenskiöldbreen and Orvindalen areas and enrichment in Sr isotopes for Nordenskiöld Land. B) $^{143}Nd/^{144}Nd_{(635\ Ma)}$ as a function of crystallization age of metavolcanic rocks from Svalbard. Samples from Orvindalen plot below the depleted mantle evolution curve and CHUR, which indicates involvement of older crust. CHUR is calculated from present day with $^{143}Nd/^{144}Nd$ of 0.512638 and $^{147}Sm/^{144}Nd$ of 0.1967 and DM was calculated from present day MORB $^{143}Nd/^{144}Nd$ of 0.5137–0.5133 and $^{147}Sm/^{144}Nd$ of 0.237 (Jacobson & Wasserberger, 1980; Allegre et al., 1983; Goldstein et al., 1984). The continental crustal endmembers were calculated from a shale with measured $^{143}Nd/^{144}Nd$ of 0.511846 and $^{147}Sm/^{144}Nd$ of 0.117 and a granulitic gneiss with $^{143}Nd/^{144}Nd$ of 0.510724 and $^{147}Sm/^{144}Nd$ of 0.0868 (Taylor et al., 1992; Nelson et al., 1993) C) Negative correlation of SiO_2 (wt%) vs. $^{143}Nd/^{144}Nd_{(635\ Ma)}$. Age correction was applied by calculating the $^{87}Rb/^{86}Sr$ and $^{147}Sm/^{144}Nd$ from the trace element concentration data for an initial age 635 Ma, based on the Torrelian unconformity. The latter is dated at ca. 640 Ma and divides older metasedimentary rocks of the Deilegga Group from younger metasedimentary rocks of the Sofiebogen Group to which the metavolcanic rocks belong (Czerny et al., 2010; Majka et al., 2014; Majka and Kosminska, 2017). The water/rock ratios were modeled from a Werenskiöldbreen sample (see Appendix 3). The fluid composition was derived from the fluid/rock partition coefficients Sr = 0.53 (650 °C; Johnson and Plank, 2000) of a Proterozoic metapelite Sr = 149 ppm (Nelson et al., 1993; Table 1). The Sr concentrations of the fluid and the rock remained constant and the fluid $^{87}Sr/^{86}Sr$ ratio decreased by 0.0015 during water–rock interaction, to simulate precipitation of Sr. Crustal endmembers are from Taylor et al. (1992), Nelson et al. (1993), Plank and Langmuir (1998) and Roddaz et al. (2007).

lowest $^{143}Nd/^{144}Nd_{(635\ Ma)}$ 0.511396–0.511781 ($\varepsilon_{Nd(635\ Ma)}$ −0.7 to −8.3). Samples from Werenskiöldbreen present a relatively wide range in $^{87}Sr/^{86}Sr_{(635\ Ma)}$ from 0.704073–0.712745, similar to rocks from Nordenskiöld Land at lower $^{143}Nd/^{144}Nd_{(635\ Ma)}$ of 0.511895–0.512148 ($\varepsilon_{Nd(635\ Ma)}$ +1.5 to +6.4) (Fig. 8A, B; Gołuchowska et al., 2012). The two samples from Chamberlindalen have $^{143}Nd/^{144}Nd_{(635\ Ma)}$ of 0.512103–0.512142 ($\varepsilon_{Nd(635\ Ma)}$ +5.6 to +6.3) and $^{87}Sr/^{86}Sr_{(635\ Ma)}$ of 0.703858–0.706110. There is a general trend of decreasing $^{143}Nd/^{144}Nd_{(635\ Ma)}$ versus SiO_2 wt% for samples from Nordenskiöld to Orvindalen (Fig. 8C).

The LILE elements, Rb and Ba, show negative trends with $^{143}Nd/^{144}Nd_{(635\ Ma)}$ for the entire sample suite (Fig. 9A, B). La concentrations and Th/La and Th/Yb ratios also show overall negative trends with $^{143}Nd/^{144}Nd_{(635\ Ma)}$ for samples from Nordenskiöld to Orvindalen (Fig. 9C, D, E). In addition, La increases with increasing $^{87}Sr/^{86}Sr_{(635\ Ma)}$ (Fig. 9F). Superimposed upon these overall trends we find that the Werenskiöldbreen samples also extend to high La and Th/La at intermediate $^{143}Nd/^{144}Nd_{(635\ Ma)}$ and low $^{87}Sr/^{86}Sr_{(635\ Ma)}$.

5. Discussion

5.1. Preservation of magmatic signals

All samples from the investigated areas of Southwest Svalbard were affected by metamorphism at greenschist to lower amphibolite facies conditions to different degrees during the Caledonian Orogeny (Hjelle et al., 1986; Dallmann et al., 1990; Czerny, 1999; Majka & Kośmińska, 2017). This has resulted in variations in the preservation of primary minerals and magmatic textures.

In contrast, the preservation of magmatic signals is recorded by the occurrence of broad trends superimposed by scatter in major element geochemistry, which indicate that the major elements have only been partly affected by metamorphism (Fig. 5). Major elements like Ti, P, Ca, Mn, Si and Al are expected to be immobile during greenschist facies metamorphism even in the presence of a fluid phase, whereas Fe, Na, K and Mg are more sensitive to metamorphism (Pearce, 1976; Winchester & Floyd, 1976; Muecke et al., 1979; MacGehan & MacLean, 1980; Motll, 1983). The greenschist facies metamorphism is shown by the presence of

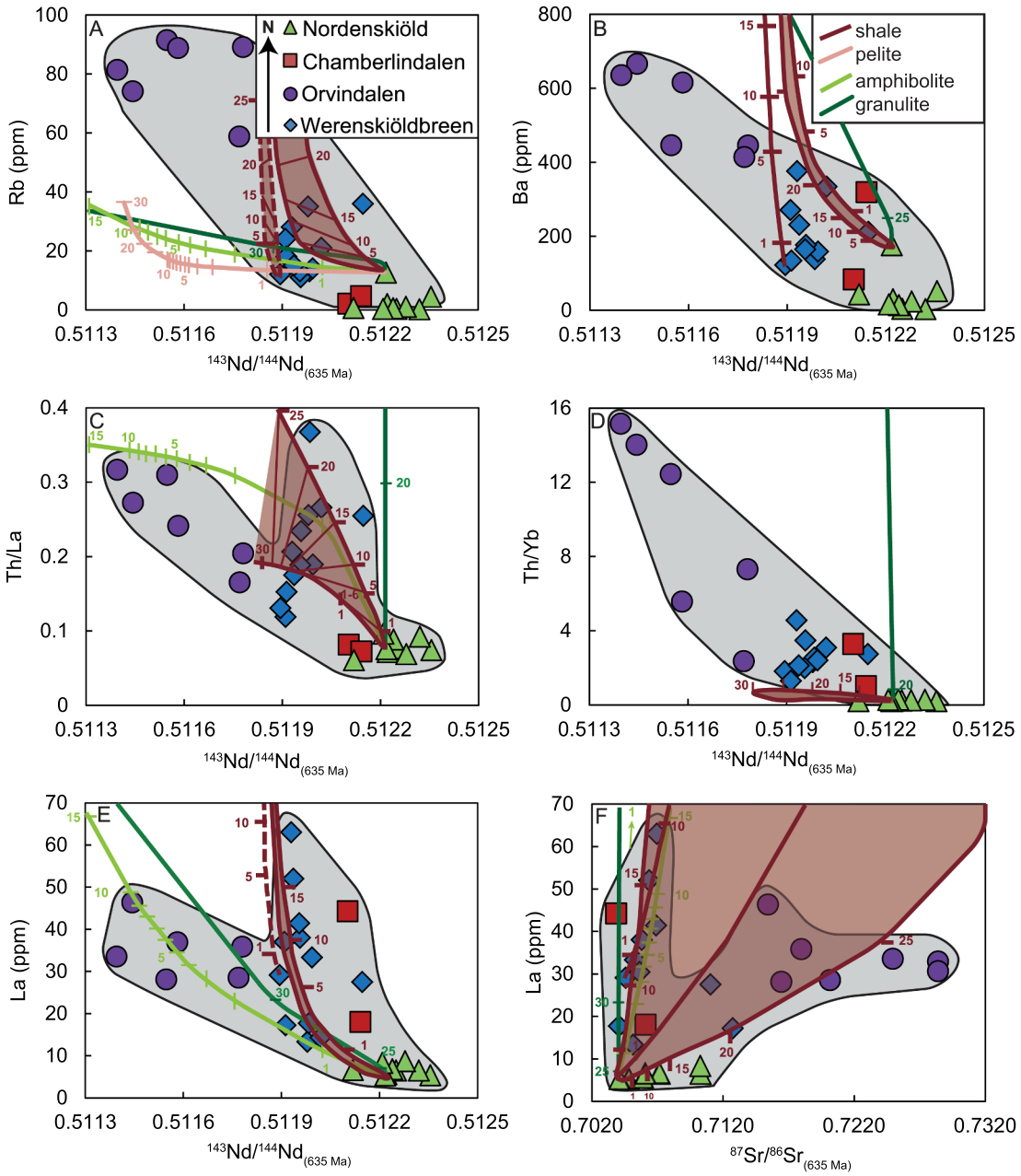

Fig. 9. Variations in trace element geochemistry with Nd and Sr isotopes. A) Rb versus $^{143}Nd/^{144}Nd_{(635\ Ma)}$, B) Ba versus $^{143}Nd/^{144}Nd_{(635\ Ma)}$, C) Th/La versus $^{143}Nd/^{144}Nd_{(635\ Ma)}$, D) Th/Yb versus $^{143}Nd/^{144}Nd_{(635\ Ma)}$, E) La versus $^{143}Nd/^{144}Nd_{(635\ Ma)}$, and F) La versus $^{87}Sr/^{86}Sr_{(635\ Ma)}$. Gray fields highlight the trends in the data. EC-AFC model curves are presented for different assimilants and for elements as data availability permits. See Appendix 3 for details of model parameters.

albite, actinolite, chlorite and epidote (Fig. 4). The influence of albite can be seen by the splitization that occurs in the metaigneous rocks from Werenskiöldbreen, Chamberlindalen and partly in Nordenskiöld Land but is absent in samples from Orvindalen (Fig. 5H; Czerny, 1999; Skelton et al., 2010; Arghe et al., 2011; Gołuchowska et al., 2012). Albite can also be observed by the high Na_2O contents in the rocks from Werenskiöldbreen and Chamberlindalen (Fig. 5F). Likewise the effects of actinolite along with epidote can be seen in wide ranges of CaO and Fe_2O_3, particularly for the Werenskiöldbreen samples. The Werenskiöldbreen samples that display high Al_2O_3 mostly show high normative orthoclase contents (3 out of 4 samples have 5–10 wt% normative orthoclase), suggesting that the high Al_2O_3 is caused by metamorphism. Chlorite and epidote are responsible for the high Al_2O_3 values in samples from Werenskiöldbreen and Chamberlindalen. Whereas the scatter within the Al_2O_3 contents for Nordenskiöld Land is likely due to the presence of garnet in some samples (Fig. 5). Additionally, K_2O contents show the effects of sericitization in the Werenskiöldbreen samples. Minor effects of metamorphism are confirmed by the normative mineral assemblages with up to 4.4 wt% secondary orthoclase in the Nordenskiöld and Chamberlindalen samples and up to 10 wt% in the Werenskiöldbreen samples (Table 1). The contrasting behavior of K_2O and Na_2O is intriguing, they are both expected to behave similarly with K_2O being more sensitive to fluid mobility. Hence the minor scatter observed in Na_2O is likely associated with the widespread albite and minor sericite, where the elevated K_2O contents in samples from Orvindalen are probably due to magmatic processes. Enrichment in TiO_2 traces the influence of rutile, titanite and Fe-Ti-oxides.

Additionally, we compare our samples to blueschists collected from the Vestgötabreen Complex, occurring in Nordenskiöld Land and Oscar

II Land, Svalbard. The greenschists and blueschists have coeval protoliths and have been metamorphosed during the Caledonian orogeny. In addition, the Caledonian metamorphism has recorded a systematic range of conditions from greenschist to blueschist with the increase in pressure demonstrated by the presence of garnet in the Nordenskiöld greenstones (Kośmińska et al., 2014). However they only show a little more scatter in major element compositions than our samples, hence, the higher grade of metamorphism does not significantly influence the major element content (Fig. 5). In detail, the blueschists from the Vestgötabreen complex, are enriched in K_2O due to phengite, Na_2O associated with glaucophane, Al_2O_3 and Fe_2O_3 due to phengite, garnet, glaucophane, hornblende and actinolite (Kośmińska et al., 2014). The blueschists have less enriched Na_2O content due to the differences in the proportions and compositions of albite and glaucophane. Therefore, the major element compositions of the greenstones from Nordenskiöld Land and Wedel Jarlsberg Land are not likely to be overly affected by metamorphism. However, the scatter in major element geochemistry may imply that the influence of metamorphism cannot be excluded despite other processes such as magma-crust interaction potentially contributing to the scatter.

The HFSE show trends of differentiation and provide evidence that these elements survived metamorphism relatively unchanged and represent magmatic signatures (Fig. 6; Gołuchowska et al., 2012). Generally REE concentrations are diluted during greenschist facies metamorphism by the formation of secondary feldspar, calcite, epidote and chlorite, producing subparallel patterns compared with fresh rock (Hopf, 1993; Zhiwei & Zhenhua 2003; Pandarinath et al., 2020). Extensive silicification is required to fractionate the HREE and produce Ce or Eu anomalies (Hopf, 1993; Zhiwei & Zhenhua 2003; Pandarinath et al., 2020). The greenschist mineral assemblages we observe show little silicification suggesting that the REE such as Nd have not been affected by the metamorphism and therefore we do not expect the $^{143}Nd/^{144}Nd_{(635\ Ma)}$ ratios to be modified. Furthermore, the Nd isotopes for the metavolcanic rocks from Southwest Svalbard have a wide range extending from $\varepsilon Nd_{(635\ Ma)}$ of −8.3 to +10.3, suggesting an unradiogenic source was involved in producing the highly negative values during magma genesis (Fig. 8B).

We also observe scatter in LILE and wide ranges of Sr isotope ratios in the metavolcanic rocks from Southwest Svalbard (Figs. 5, 6 and 8). Notably, the Nd isotopes correlate with relatively fluid immobile and incompatible trace element ratios such as Th/Yb and Th/La as well as the LILE elements Rb and Ba (Fig. 9). The correlation between Nd isotopes and Rb and Ba concentrations provide strong evidence for incorporation of crustal materials or enriched sources in the magma opposed to metamorphism as the dominant control on the LILE geochemistry.

Given the high mobility of the LILE some influence of metamorphism would be expected (Ridley, 2012). Common effects of metamorphism on metabasalts are loss of LILE, opposed to gain as we observe in Fig. 6 (Zack & John, 2007). This is due to the metamorphic assemblage formed, where the dominant mineral is chlorite that does not host LILE, leaving minor amphibole to take up Rb and Ba and the rare epidote to carry Sr. Furthermore, the Vestgötabreen Complex blueschists contrast in trace element composition to the greenschist metavolcanic rocks with the same protolith. This contrast is especially visible for the LILE such as Sr, which are depleted in the blueschists, consistent with loss of LILE due to metamorphism (Fig. 6; Zack & John, 2007). This observation emphasizes the behavior of LILE as the metamorphic grade increases. Typically in blueschists processes affecting the mobile elements such as Sr are leaching opposed to exchange or addition from the metamorphic fluids. The composition of the blueschists likely reflects the progressive influence of metamorphism as the metamorphic grade increases during subduction associated with the Caledonian orogeny. These compositions contrast with the greenschist facies metavolcanic rocks and suggest the preservation of magmatic signatures at the lower metamorphic grades recorded by our samples (Figs. 6 and 7).

It is also possible that the $^{87}Sr/^{86}Sr_{(635\ Ma)}$ ratio of Southwest Svalbard's rocks could be modified towards ratios of the fluid in contrast to the immobile $^{143}Nd/^{144}Nd_{(635\ Ma)}$ ratio (Pfänder et al., 2002; Barker et al., 2008). The overall negative trend between $^{87}Sr/^{86}Sr_{(635\ Ma)}$ and $^{143}Nd/^{144}Nd_{(635\ Ma)}$ is consistent with a primary magmatic signature. However, we consider the possibility of the elevated Sr isotope ratios of the metavolcanic rocks being influenced by metasomatic fluids originating from high $^{87}Sr/^{86}Sr$ pelitic assemblages (Nelson et al., 1993). During metamorphism Rb and Ba are leached from metapelites but Sr is deposited in metapelites, therefore metasomatic fluids in equilibrium with pelitic assemblages are rich in Rb and Ba and poor in Sr (Masters & Ague, 2005). A Sr poor fluid is likely to leach Sr from the rock and therefore the influence on the Sr isotope ratio of the rock will be limited. At low water/rock ratios massive rocks, such as those found in Southwest Svalbard, display altered minerals. However, fluids mainly precipitate in veins and increasing water/rock ratios to ca. 10 leads to vein networks. Additionally water/rock ratios of >50 are associated with channelized fluid flow through fault zones (Masters & Ague, 2005; Zack & John, 2007; Barker et al., 2010).

We have modeled the water/rock ratios for Rb and Sr concentrations as well as for Sr isotopes using fluid/rock partitioning from Johnson & Plank (2000) and a Proterozoic metapelite (Table 1; Nelson et al., 1993). The model is based on a simple mass balance between fluid and rock endmembers, where the fluid endmember has inherited 43 ppm Rb and 79 ppm Sr from the metapelite. Since it is not possible to constrain the timing of such a metasomatic event, we have not accounted for radiogenic ingrowth in the model. The sample compositions can be explained by water/rock ratios that range from as low as 5 up to 100 (Figs. 6 and 8). Significant fluid metasomatism on the order of more than 10:1 would be required to produce the elevated Rb and Sr concentrations and Sr isotope ratios (Figs. 6 and 8). Such high water/rock ratios would be evident in intense veining of the outcrops, which is not observed in the field (Fig. 3). However, it is possible that fluid metasomatism superimposed minor effects on the already elevated LILE and Sr isotope ratios.

Additionally, the samples with the most intense metamorphism from Nordenskiöld Land display the lowest $^{87}Sr/^{86}Sr_{(635\ Ma)}$ of 0.70411–0.71028 (Fig. 8A). However, even these samples from Nordenskiöld Land, extend to relatively high $^{87}Sr/^{86}Sr_{(635\ Ma)}$ up to 0.71028, which could be caused by crustal assimilation in the magmatic system rather than the influence of fluid metamorphism.

Finally, carbon isotopes are known to be sensitive to metamorphic fluid activity both due to thermally induced fractionation and due to contrasting fluid composition (Skelton et al., 2015). However the carbonates from the Sofiebogen group in northwestern Wedel Jarlsberg Land have $\delta^{13}C$ of −5.5 to −3.1‰ hence, they exhibit undisturbed C-isotope excursions that correlate with the Snowball Earth event at 635 Ma (Wala et al., 2021). These carbonates are found in the same stratigraphic sequence as the metavolcanic rocks presented here and were therefore metamorphosed together. Hence the preservation of carbon isotope signature provides further evidence for a limited influence of metamorphism on the rock geochemistry.

5.2. Signatures of crustal assimilation

From the four areas, we observe trends of decreasing incompatible elements such as La and Nd from South (Werenskiöldbreen) to North (Nordenskiöld Land) (Fig. 6). An exception occurs at Orvindalen, which is situated North of Werenskiöldbreen. The samples from Orvindalen have similar geochemistry to rocks from the adjacent Werenskiöldbreen area, however several of them display higher contents of Th, La, Th/Yb and Nb/Yb relative to other immobile elements (Fig. 9B, C). In general, samples from the Werenskiöldbreen and Orvindalen areas extend towards incompatible element compositions of sedimentary upper crust (Fig. 7), whereas samples from Nordenskiöld Land and Chamberlindalen have compositions indicating much less interaction with the crust. In addition, the massive nature of the outcrops in Nordenskiöld Land, Chamberlindalen and Werenskiöldbreen is consistent with formation by

magmatic processes that occurred prior to eruption. In contrast metamorphic or metasomatic processes responsible for such geochemical modification would result in highly veined outcrops (Masters & Ague, 2005; Zack & John, 2007). Therefore the massive outcrops are inconsistent with post-magmatic hydrothermal modification of the metavolcanic rocks, instead the field textures support the role of assimilation of crustal materials in controlling the geochemistry (Fig. 3).

Comparing the trace element geochemistry of the metavolcanic rocks from Nordenskiöld Land and Chamberlindalen, along with the Vestagötabreen Complex blueschists we observe that they are similar to North Atlantic MORB (Figs. 10 and 11). In contrast the samples from Werenskiöldbreen and Orvindalen often start near to the MORB and extend to elevated Th/La, Th/Nb, and La/Nb (Figs. 10 and 11). These observations are confirmed by ΔNb (Fitton et al., 1997), where the Nordenskiöld Land and Werenskiöldbreen samples have slightly negative to neutral ΔNb, and are thereby similar to MORB (Fig. 10d). In contrast, samples from Chamberlindalen and Orvindalen extend to positive values of ΔNb, indicating another source. The scatter in trace elements and wide range in Sr isotopes within each suite, are associated with unradiogenic Nd isotope compositions especially at Werenskiöldbreen and Orvindalen. These geochemical signatures are characteristic of crustal assimilation and unlike the more systematic variations expected from source heterogeneity.

Metavolcanic rocks from Southwest Svalbard occur within thick sequences of metasedimentary rocks (Ohta, 1985; Hjelle et al., 1986; Bjørnerud, 1990; Dallmann et al., 1990; Czerny, 1999; Bjørnerud, 2010). The presence of metasedimentary crust combined with elevated Rb, Ba, Sr, Th, La and Sr-Nd isotopes suggest a role for crustal assimilation in the magma. To determine the role of magma-crust interaction, we have applied the Energy Constrained Assimilation and Fractional Crystallization (EC-AFC) model of Bohrson & Spera (2007). We modeled assimilation of a wide variety of upper and lower crustal lithologies with a primary magma represented by a sample from Nordenskiöld Land. The Nordenskiöld Land sample with the lowest $^{87}Sr/^{86}Sr_{(635\ Ma)}$ was selected as a parental magma (Appendix 3). The modeling was performed for Sr, Nd, Rb, Ba, Th, Nb, La and Yb concentrations and Sr and Nd isotope ratios depending on data availability (See Appendix 3 for end member compositions). Bulk partition coefficients for basaltic magma, shale, upper and lower crust were estimated from partition coefficients given by Beattie (1994), Bindeman and Davis (2000), Ewart and Griffin (1994), Mahood and Hildreth (1983), McKenzie and O'Nions (1991), Sobolev et al. (1996) (Appendix 3). Thermal and equilibrium conditions of the magma are also given in Appendix 3. Lacking geochemical data or samples from the local crustal lithologies, the crustal endmembers were selected from Proterozoic rocks from the Arctic area, such as Greenland and Alaska, where possible (Taylor et al., 1992; Nelson et al., 1993). Other lithologies were taken from global compilations (Plank & Langmuir, 1998; Rudnik & Gao, 2003). All contaminants were age corrected to 635 Ma to give the isotopic ratios at the time of the magmatism in Southwest Svalbard. Neoproterozoic shale, metapelite and modern carbonate were chosen as possible upper crustal contaminants (Nelson et al., 1993; Plank & Langmuir, 1998; Roddaz et al., 2007). To test for lower crustal lithologies granulite gneiss and amphibolite from East Greenland have been employed (Taylor et al., 1992).

Next we consider the effects of magma-crust interaction for Wedel Jarlsberg Land and specifically the geochemistry of samples from Werenskiöldbreen and Chamberlindalen. We observe elevated trace element compositions of Rb < 35 ppm, Ba < 400 ppm, Sr < 360 ppm, Th

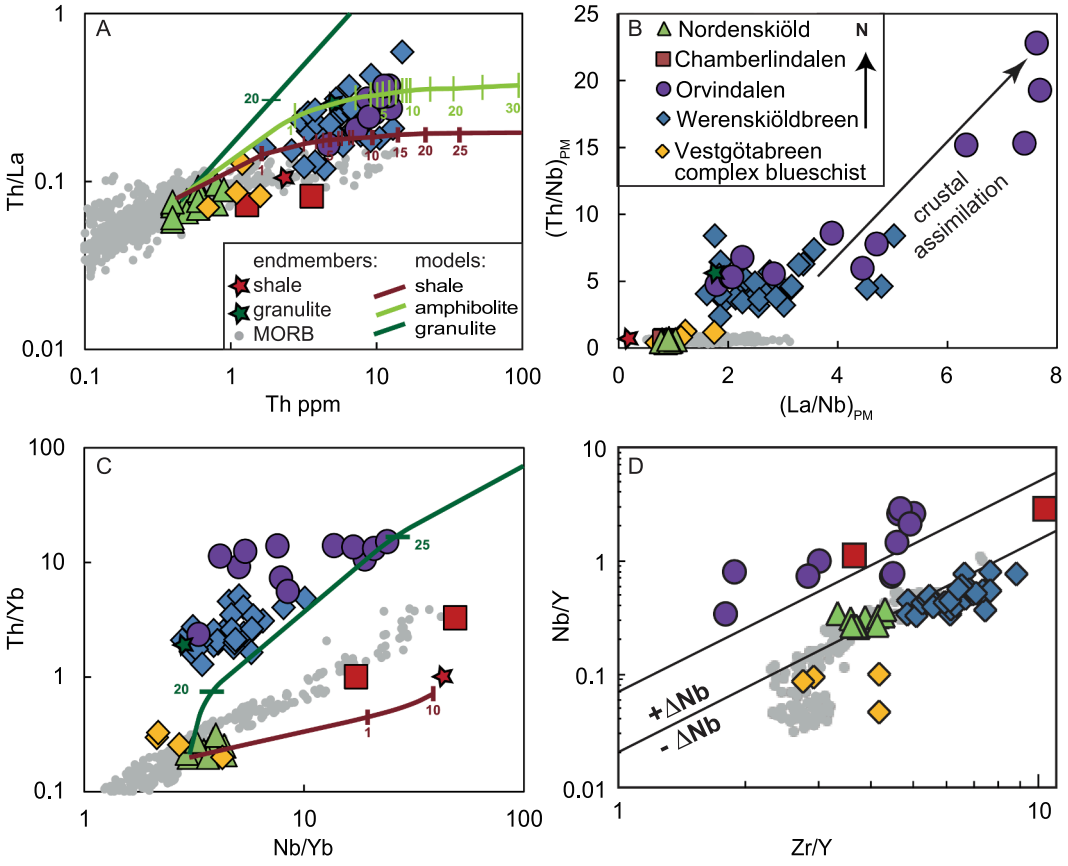

Fig. 10. Trace element ratios for rocks from Werenskiöldbreen, Orvindalen, Chamberlindalen and Nordenskiöld Land indicating crustal contamination for rocks from the South of Wedel Jarlsberg Land. ΔNb after Fitton et al. (1997). MORB compositions are from le Roux et al. (2002a–c), le Roux (2000), Marshall et al. (2017), Truong et al. (2018). Crustal endmembers are from Taylor et al. (1992), Nelson et al. (1993), Plank and Langmuir (1998) and Roddaz et al. (2007). Model curves present EC-AFC of shale, carbonate, amphibolite and granulite lithologies with the magmas (See Appendix 3 for model parameters).

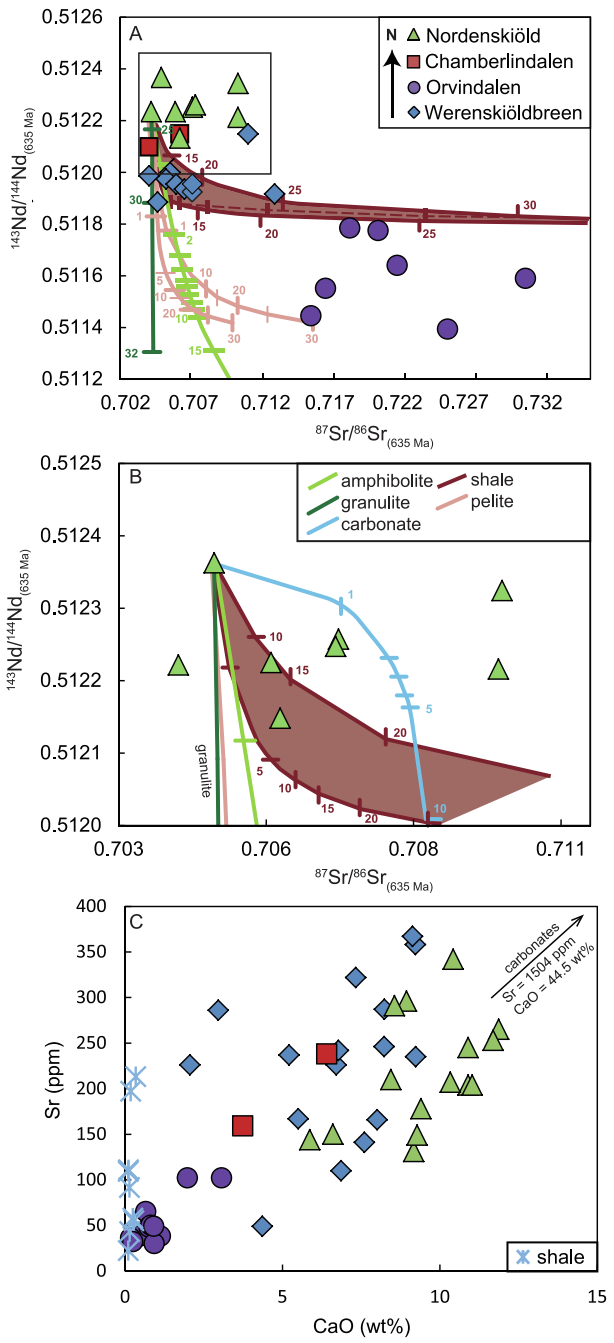

Fig. 11. A) EC-AFC models to explain the Sr and Nd isotope compositions of rocks from Werenskiöldbreen, Orvindalen, Chamberlindalen and Nordenskiöld Land. Inset marks the area shown in B. Color coded numbers by model lines denote the proportion of assimilation as percentages. B) EC-AFC models for rocks from Nordenskiöld Land. C) Increasing trend of Sr ppm vs. CaO wt% indicates assimilation of Sr-rich carbonate minerals (after Plank & Langmuir, 1998). For comparison, shale is added (Roddaz et al., 2007). Carbonates exceed the scale and they are marked by an arrow. Sr and Nd isotopes of contaminants were age corrected to 635 Ma. Proterozoic shale (Roddaz et al., 2007), metapelite (Nelson et al., 1993), granulite and amphibolite (Taylor et al., 1992) and carbonate (Plank & Langmuir, 1998) have been used as crustal end-members for the EC-AFC model (Bohrson & Spera, 2001, 2007; Spera & Bohrson, 2001; see Appendix 3 for more details).

< 13 ppm, and La < 65 ppm as well as $^{87}Sr/^{86}Sr_{(635\ Ma)}$ of up to 0.7127. These enrichments introduce scatter taking the samples away from trends of fractional crystallization (Figs. 6, 8, 9, 10). A suitable crustal assimilant such as shale would have high, Rb, Ba, Sr, La, Th and $^{87}Sr/^{86}Sr_{(635\ Ma)}$ (Fig. 9E; Roddaz et al., 2007). These characteristics can be modeled by assimilation of 15–20% shale (Figs. 9, 10, 11). Assimilation of shale is consistent with the occurrence of corundum in the normative mineralogy and also with the phyllites found in the Sofiebogen, Recherchebreen and Dunderbukta sequences (Table 1; Fig. 2). There are a few aspects of the samples that are difficult to explain by assimilation of shale alone, such as high Th/Yb (Figs. 9 & 10). In the samples from Chamberlindalen we observe high Th/Yb at high Nb/Yb following the MORB field (Fig. 10C) as well as positive ΔNb (Fig. 10D). This suggests that these samples have a more enriched source, which has likely interacted with the shale assimilant. In contrast, the Werenskiöldbreen samples have negative ΔNb comparable to MORB, the lower Th/La ratios also compare well with MORB compositions, however the high Th/Yb could be a feature of a source, which then assimilates shale (Fig. 10). Alternatively, the high Th/Yb is similar to signatures produced by assimilation of granulite and Th/La is also elevated in amphibolite and granulite gneiss (Figs. 9 and 10; Taylor et al., 1992). Models suggest assimilation on the order of 20–30% granulite or a few percent amphibolite would be required to produce these compositions. It is most likely that both source variations and granulite or amphibolite assimilation are involved, for instance, if Th is filtered to remove high values that deviate from the differentiation trend (Fig. 6E), the trend of decreasing Th/Yb and $^{143}Nd/^{144}Nd_{(635\ Ma)}$ remains (Fig. 9D). This trend can be explained by two sources or assimilation with a low $^{143}Nd/^{144}Nd_{(635\ Ma)}$, low Th/Yb shale. Only two samples are not explained by this trend and they are probably influenced by assimilation of granulite or amphibolite in the lower crust. The stratigaphic record also shows the presence of amphibolite and paragneiss in the Eimfjellet Complex and Isbjørnhamna Group (Fig. 2).

At Orvindalen, we observe the most enriched signatures extending to low $^{143}Nd/^{144}Nd_{(635\ Ma)}$, at high K_2O, Rb, Ba, Th and $^{87}Sr/^{86}Sr_{(635\ Ma)}$. The high Rb, Ba and $^{87}Sr/^{86}Sr_{(635\ Ma)}$ can be explained by up to 30% assimilation of a shale component (Figs. 5, 8, 9, 10, 11; Roddaz et al., 2007). Likewise, we observe corundum in the normative mineralogy for these samples confirming the interaction with an Aluminium rich shale lithology (Table 1). The Orvindalen samples were collected from tuff deposits that contain varying proportions of epiclastic materials (30–80%), including tourmaline derived from shale as well as carbonate minerals. The significant contribution and dominantly pelitic nature of these epiclastic materials suggests that the geochemical signature of the Orvindalen tuff was at least in part generated by mechanical mixing with the high Nb/Yb and $^{87}Sr/^{86}Sr_{(635\ Ma)}$ of a shale during the explosive eruption. Again we find some features that are not readily explained by assimilation of shale, such as the low $^{143}Nd/^{144}Nd_{(635\ Ma)}$ versus intermediate La, high Th/La and Th/Yb ratios (Figs. 8, 9, 10, 11). Even if we take source variations into consideration by considering the highest $^{143}Nd/^{144}Nd_{(635\ Ma)}$ as the source, it is hard to reproduce this data by assimilation of shale alone. These signatures can be explained by assimilation of amphibolite or granulite gneiss (Figs. 9, 10, 11; Taylor et al., 1992). Approximately 10% amphibolite compared to <30% granulite would be required to reproduce these geochemical relationships. For some elements such as Rb and Ba with $^{143}Nd/^{144}Nd_{(635\ Ma)}$, the Orvindalen samples plot between shales and amphibolite-granulite compositions. However the shales may indeed have more varied compositions as illustrated by the Rb and $^{143}Nd/^{144}Nd_{(635\ Ma)}$ assimilation model of metapelite (Fig. 9A). Thus the local shale may well produce assimilation trends between those of the shale and metapelite employed here.

The metavolcanic rocks from Nordenskiöld Land have a less obvious influence of crustal contamination, because of the relatively high $^{143}Nd/^{144}Nd_{(635\ Ma)}$ ratios and HFSE compositions. This indicates that they are only weakly contaminated in comparison to the rest of the samples from Southwest Svalbard (Figs. 6, 9 & 11). Samples collected from Nordenskiöld Land have relatively high Sr and low Th contents (Figs. 6, 7), at a wide range of $^{87}Sr/^{86}Sr_{(635\ Ma)}$ from 0.70411 to 0.71028. We consider these geochemical variations to be significant and beyond

the likely effects of metamorphism, which would also have affected Rb and Ba. Therefore minor magma-crust interaction likely resulted in the elevated Sr and $^{87}Sr/^{86}Sr_{(635\ Ma)}$ (Fig. 6C & Fig. 11B; Taylor et al., 1992; Plank & Langmuir, 1998; Rudnick & Gao, 2003). According to Plank and Langmuir (1998), Sr can be easily accumulated in carbonates, because it substitutes for Ca in calcite. Sr also occurs in high concentrations in nanofossil and carbonate oozes (1500–2000 ppm for modern carbonate oozes; Plank & Langmuir, 1998), which implies that in sediments the abundance of Sr depends on the proportion of calcium carbonate, clays and biogenic opal. We observe a positive correlation of Sr with CaO, trending towards carbonate compositions (Fig. 11C). Hence, we decided to consider assimilation of carbonate with the EC-AFC model. Several samples from Nordenskiöld Land can realistically be explained by approximately 2% carbonate assimilation or 15% shale assimilation (Fig. 11B). Furthermore, in Nordenskiöld Land, the local crust is dominated by carbonates, but in places interbedded carbonate (limestone, marble, dolomites) and phyllite are exposed making a combination of carbonate and shale available (Hjelle, 1962; 1967; Dallmann et al., 2015). Neoproterozoic carbonates from Svalbard and globally have an average of $^{87}Sr/^{86}Sr$ 0.7070–0.7090 (Derry et al., 1989; Cox et al., 2016; Wala et al., 2021). The relatively low $^{143}Nd/^{144}Nd$ in the carbonate assimilant compared to the Nordenskiöld Land samples is confirmed by estimates of Arctic carbonates during the Neoproterozoic having similarly low $^{143}Nd/^{144}Nd$ as well as globally in the oceans (Tütken et al., 2002; Cox et al., 2016). Despite low Nd concentrations limiting the effect of assimilation on magma $^{143}Nd/^{144}Nd$, the low $^{143}Nd/^{144}Nd$ of carbonates exerts some influence on the assimilation curves. Consequently, the whole range of Sr-Nd isotope ratios for all of the Nordenskiöld Land samples is difficult to explain by assimilation alone. Alternative explanations include partial melting of the more fertile components in the pelitic assemblages to preferentially enrich the magma in crustally derived Sr over Nd (Duffield & Ruiz, 1998). A minor component of metamorphism could also contribute to the elevated Sr isotope composition.

To summarize, the metavolcanic rocks from Wedel Jarlsberg Land are consistent with magma-crust interaction of a lower crustal granulite or amphibolite. Additionally, samples from Werenskiöldbreen suggest assimilation of 15–20% upper crustal shale. The Orvindalen samples also indicate assimilation and mechanical mixing with shale during eruption. For Nordenskiöld Land, the elevated Sr isotope ratios are difficult to explain, however the models suggest small amounts of carbonate assimilation could contribute. In addition, post-magmatic hydrothermal alteration or metamorphism may have modified the geochemical characteristics produced by magma-crust interaction.

5.3. *The relationship between magma-crust interaction and the Neoproterozoic crust*

Here, we consider the Neoproterozoic crust and the influence it would have had on magma evolution and magma-crust interaction. The stratigraphic record shows a change from phyllite dominated to interlayered carbonate-phyllite and carbonate dominated assemblages from

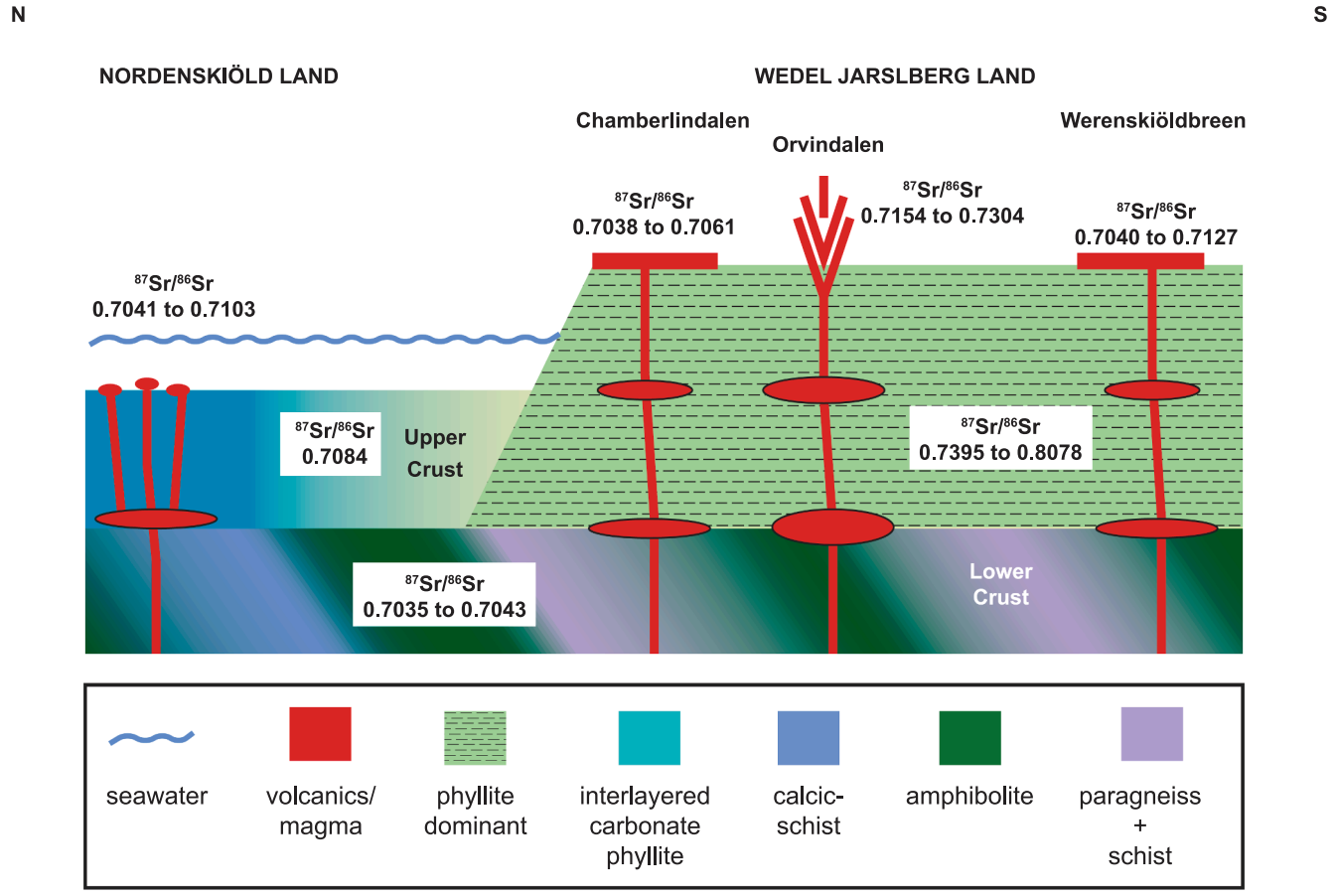

Fig. 12. Schematic illustration of the petrogenesis of metavolcanic rocks erupted at Werenskiöldbreen, Orvindalen, Chamberlindalen and Nordenskiöld Land. The upper and lower crustal transition provides a density contrast promoting magma storage and magma-crust interaction with lower crustal granulite gneisses and amphibolites. Magmas ascending through the upper crust come into contact with impermeable layers of pelitic shale causing magma stagnation and crustal assimilation. At Werenskiöldbreen and Chamberlindalen the eruptions are subaerial and effusive, whereas at Orvindalen the magmas are more evolved and erupt explosively inducing mechanical mixing with the surrounding pelitic shales and carbonates. In Nordenskiöld Land, submarine eruptions are effusive forming pillow lavas; the marine setting provides more carbonate for magma-crust interaction than elsewhere.

Wedel Jarlsberg Land to Nordenskiöld Land (Fig. 2; Hjelle, 1962, 1967; Birkenmajer, 1975; Krasil'shchikov et al., 1979; Hjelle et al., 1986; Bjørnerud, 1990; Dallmann et al., 1990; Czerny et al., 1993). Hence, the shift away from phyllite dominated sequences to more carbonate components correspond to the change in nature and extent of crustal assimilation we observe between the metavolcanic rocks on Wedel Jarlsberg Land and Nordenskiöld Land. The continental crust may also have been subjected to syndepositional faulting, which would create pathways to focus magma flow and decrease the exposure to and interaction with the crust. The metavolcanic rocks from Wedel Jarlsberg Land show the influence of magma-crust interaction in the lower crust, associated with granulite or amphibolite components, which connect with the paragneisses and amphibolite found within and beneath the Eimfjellet group in the Werenskiöldbreen area (Fig. 2). This observation suggests that the paragneisses and amphibolites were present at lower crustal depths beneath most of Wedel Jarlsberg Land, as confirmed by the occurrence of lower crustal seismic velocities throughout the area (Sellevoll et al., 1991; Czuba et al., 1999; Ritzmann et al., 2002, 2004). The contact between lower crust and upper crust would likely have provided a density contrast that promoted magma storage and associated assimilation. Likewise the density difference between the upper mantle and lower crust would probably have caused magma storage in the lower crust, potentially promoting assimilation of amphibolite or granulitic gneiss (Fig. 12). Magma-crust interaction in the lower crust is consistent with Gołuchowska et al. (2016), who found that the main level of magma storage for alkaline magmatism in the Chamberlindalen area was near the base of the crust. Another obstacle to magma ascent in the Neoproterozoic crust of Wedel Jarlsberg Land is the impermeable phyllites found in the Sofiebogen, Recherchebreen and Dunderbukta groups (Fig. 2). These impermeable layers would probably have facilitated magma storage and associated interaction between the magma and shale (phyllite protolith) (Fig. 12).

Volcanism on Wedel Jarlsberg Land was subaerial whereas in Nordenskiöld Land, pillow lavas erupted in a submarine setting (Fig. 2; Ohta, 1985; Hjelle et al., 1986; Bjørnerud, 1990; Dallmann et al., 1990). The eruption of pillow lavas in Nordenskiöld Land is consistent with rifting and the formation of a marine basin, where carbonates dominate and are interlayered with terrestrially derived shales. The ascending magma only interacted to a limited extent with these carbonate and shale successions before eruption at the sea floor (Fig. 12). Furthermore, at Orvindalen the volcanism was explosive forming tuff deposits that contain varying degrees of epiclastic materials (30–80%), derived directly from shale and carbonate lithologies. The significant contribution of such epiclastic materials accounts for the high proportions of shale involved in the genesis of the Orvindalen tuff. This can be explained by mechanical mixing with phyllites and minor carbonate components during and following the explosive eruption (Figs. 9, 10, 11 & 12). The overall higher levels of assimilation likely contribute to the more felsic magma compositions and explosivity, potentially aided by the presence of groundwater.

6. Conclusion

Despite the effects of metamorphism, we show that the compositions of the Neoproterozoic metavolcanics from Southwest Svalbard are dominantly magmatic. The metavolcanic rocks from Werenskiöldbreen and Orvindalen record assimilation of granulite and amphibolite lithologies in the lower crust. During ascent through the upper crust the Wedel Jarlsberg Land and Nordenskiöld Land magmas have undergone assimilation with shale and carbonate to variable degrees. The tuffs from Orvindalen preserve evidence for mechanical mixing with phyllite and carbonate during eruption, which is consistent with the geochemical signature of significant assimilation of shale.

CRediT authorship contribution statement

Karolina Gołuchowska: Investigation, Visualization, Writing – original draft, Funding acquisition. **Abigail K. Barker:** Conceptualization, Writing – review & editing, Supervision, Funding acquisition. **Maciej Manecki:** Conceptualization, Writing – review & editing, Supervision, Funding acquisition. **Jarosław Majka:** Conceptualization, Writing – review & editing, Funding acquisition. **Karolina Kośmińska:** Investigation, Writing – review & editing. **Robert M. Ellam:** Validation, Writing – review & editing. **Jakub Bazarnik:** Investigation, Validation, Writing – review & editing. **Karol Faehnrich:** Visualization, Writing – review & editing. **Jerzy Czerny:** Resources.

Declaration of Competing Interest

The authors declare that they have no known competing financial interests or personal relationships that could have appeared to influence the work reported in this paper.

Acknowledgements

We would like to thank all of the scientists who participated in the many polar expeditions to Wedel Jarlsberg Land and Nordenskiöld Land, Svalbard, under the leadership of Andrzej Manecki, Jerzy Czerny and Henning Lorenz. This work would never have been possible without their support for organization of expeditions, geological observations and sample collection. We thank Anne Kelly, Valerie Olive, Vincent Gallagher and Terry Donnelly from SUERC, Scotland for help in preparation of samples for isotope geochemistry and very valuable discussions. We are grateful to Charles Beard for constructive discussions of this manuscript and to Jussi Heinonen and two anonymous reviewers for their valuable comments. Thanks also goes to Christian Schiffer for discussions concerning the crustal structure in this area. Financial support for the research was provided by the Polish National Science Centre (NCN) grant, No. 2012/05/N/ST10/03594 to K. Gołuchowska and a Swedish Royal Academy (KVA) grant to J. Majka. This research was also supported by internal funding from the Polish Geological Institute (NRI) grant No. 62.9012.2015.00.0 to J. Bazarnik. In addition, fieldwork was supported by AGH University of Science and Technology, Poland and the NOA project grant from the Polarforskningsekretariet, Sweden.

Appendix A. Supplementary material

Supplementary data to this article can be found online at https://doi.org/10.1016/j.precamres.2021.106521.

References

Allègre, C.J., Hart, S.R., Minster, J.-F., 1983. Chemical structure and evolution of the mantle and continents determined by inversion of Nd and Sr isotopic data, II. Numerical experiments and discussion. Earth Planet. Sci. Lett. 66, 191–213.

Anczkiewicz, R., Platt, J.P., Thirlwall, M.F., Wakabayashi, J., 2004. Franciscan subduction off to a slow start: evidence from high precision Lu-Hf garnets ages on high grade-blocks. Earth Planet. Sci. Lett. 225, 147–161.

Anczkiewicz, R., Thirlwall, M.F., 2003. Improving precision of Sm-Nd garnet dating by H_2SO_4 leaching: a simple solution to the phosphate inclusion problem. Geological Society, London, Special Publications 220 (1), 83–91.

Arghe, F., Skelton, A., Pitcairn, I., 2011. Spatial coupling between spilitization and carbonation of basaltic sills in SW Scottish Highlands: evidence of a mineralogical control of metamorphic fluid flow. Geofluids 11 (3), 245–259.

Balashov, Y.A., Larionov, A.N., Gannibal, L.F., Sirotkin, A.N., Teben'kov, A.M., Ryüngenen, G.I., Ohta, Y., 1993. An Early Proterozoic U-Pb zircon age from an Eskolabreen Formation gneiss in southern Ny Friesland, Spitsbergen. Polar Res. 12, 147–152.

Balashov, J.A., Teben'kov, A.M., Ohta, Y., Larionov, A.M., Sirotkin, A.N., Gannibal, L.F., Ryungenen, G.I., 1995. Grenvillian U-Pb zircon ages of quartz porphyry and rhyolite clasts in a metaconglomerate at Vimsodden, southwestern Spitsbergen. Polar Res. 14 (3), 291–302.

Balashov, Y.A., Peucat, J.J., Teben'kov, A.M., Ohta, Y., Larionov, A.N., Sirotkin, A.N., Bjørnerud, M., 1996. Rb-Sr whole rock and U-Pb zircon datings of the granitic-

gabbroic rocks from Skålfjellet Subgroup, southwest Spitsbergen. Polar Res. 15, 167–181.
Barker, A.K., Coogan, L.A., Gillis, K.M., Weis, D., 2008. Strontium isotope constraints on fluid flow in the sheeted dike complex of fast spreading crust: pervasive fluid flow at Pito Deep. Geochem. Geophys. Geosyst. 9 (6), 1–19.
Barker, A.K., Coogan, L.A., Gillis, K.M., Hayman, N.W., Weis, D., 2010. Direct observation of a fossil high-temperature, fault-hosted, hydrothermal upflow zone in crust formed at the East Pacific Rise. Geology 38 (4), 379–382. https://doi.org/10.1130/G30542.110.1130/2010096.
Barnes, C.J., Schneider, D.A., 2019. Late Cretaceous−Paleogene burial and exhumation history of the Southwestern Basement Province, Svalbard, revealed by zircon (U-Th)/He thermochronology. In Piepjohn, K., Strauss, J.V., Reinhardt, L., and McClelland, W.C., (Eds.), Circum-Arctic Structural Events: Tectonic Evolution of the Arctic Margins and Trans-Arctic Links with Adjacent Orogens. Geological Society of America Special Paper 541, p. 1–22, Doi: 10.1130/2018.2541(07).
Barnes, C., Majka, J., Schneider, D.A.S., Walczak, K., Bukała, M., Kośmińska, K., Tokarski, T., Karlsson, A., 2019. High-spatial resolution dating of monazite and zircon reveals the timing of subduction–exhumation of the Vaimok Lens in the Seve Nappe Complex (Scandinavian Caledonides). Contrib. Miner. Petrol. 174, 5. https://doi.org/10.1007/s00410-018-1539-1.
Barnes, C.J., Walczak, K., Janots, E., Schneider, D., Majka, J., 2020. Timing of paleozoic exhumation and deformation of the high-pressure vestgötabreen complex at the motalafjella Nunatak, Svalbard. Minerals 10 (2), 125.
Beattie, P., 1994. Systematics and energetics of trace-element partitioning between olivine and silicate melts: Implications for the nature of mineral/melt partitioning. Chem. Geol. 117 (1-4), 57–71. https://doi.org/10.1016/0009-2541(94)90121-X.
Bernard-Griffiths, J., Peucat, J.J., Ohta, Y., 1993. Age and nature of protoliths in the Caledonian blueschist-eclogite complex of western Spitsbergen: a combined approach using U-Pb, Sm-Nd and REE whole-rock systems. Lithos 30 (1), 81–90.
Bindeman, I.N., Davis, A.M., 2000. Trace element partitioning between plagioclase and melt: Investigation of dopant influence on partition behavior. Geochim. Cosmochim. Acta 64 (16), 2863–2878. https://doi.org/10.1016/S0016-7037(00)00389-6.
Birkenmajer, K., 1975. Caledonides of Svalbard and plate tectonics. Bull. Geol. Soc. Den. 24, 1–19.
Bjørnerud, M., 1990. An Upper Proterozoic unconformity in northern Wedel Jarlsberg Land, southwest Spitsbergen: lithostratigraphy and tectonic implications. Polar Res. 8 (2), 127–139.
Bjørnerud, M.G., 2010. Stratigraphic record of Neoproterozoic ice sheet collapse: the Kapp Lyell diamictite sequence, SW Spitsbergen. Svalbard Geol. Mag. 147 (3), 380–390.
Bohrson, W.A., Spera, F.J., 2007. Energy-constrained recharge, assimilation, fractional 2 crystallization (EC-RAχFC): a visual basic computer code for 3 calculating trace element and isotope characteristics of open-4 system magmatic systems 5.
Bohrson, W.A., Spera, F.J., 2001. Energy-constrained open-system magmatic processes II: application of energy-contrained assimilation-fractional crystallization (EC-AFC) model to magmatic system. J. Petrol. 42, 1019–1041.
Condon, D., Zhu, M., Bowring, S., Wang, W., Yang, A., Jin, Y., 2005. U-Pb ages from the Neoproterozoic Doushantuo Formation, China. Science 308 (5718), 95–98.
Cox, G.M., Halverson, G.P., Stevenson, R.K., Vokaty, M., Poirier, A., Kunzmann, M., Li, Z. X., Denyszyn, S.W., Strauss, J.V., Macdonald, F.A., 2016. Continental flood basalt weathering as a trigger for Neoproterozoic Snowball Earth. Earth Planet. Sci. Lett. 446, 89–99. https://doi.org/10.1016/j.epsl.2016.04.016.
Czerny, J., Kieres, A., Manecki, M., Rajchel, J., 1993. Geological map of the SW part of Wedel Jarlsberg Land. In: Manecki, A. (Ed.), Spitsbergen, 1:25 000. Institute of Geology and Mineral Deposits AGH, Cracow, pp. 1–61.
Czerny, J., 1999. Petrogenesis of metavolcanites of the southern part of Wedel Jarlsberg Land (Spitsbergen). Prace Mineralogiczne 86, Wydawnictwo Oddzialu PAN, Krakow.
Czerny, J., Majka, J., Gee, D.G., Manecki, M., Manecki, A., 2010. Torellian Orogeny: evidence of a Late Neoproterozoic tectonothermal event in southwestern Svalbard's Caledonian basement. NGF Abstr. Proc. 35–36.
Czuba, W., Grad, M., Guterch, A., 1999. Crustal structure of north-western Spitsbergen from DSS measurements. Polish Polar Res. 20 (2), 131–148.
Dallmann, W.K., Hjelle, A., Ohta, Y., Salvigsen, O., Maher, H.D., Bjørnerud, M., Hauser, E.C., Craddock, C., 1990. Geological map of Svalbard 1: 100,000, Van Keulenfjorden. With description. Norsk Polarinstitutt Temakart, No. 15.
Dallmann, W., Elvevold, S., Majka, J., Piepjohn, K., 2015. Tectonics and Tectonothermal events. In: Geoscience Atlas of Svalbard. Norwegian Polar Institute, Tromso, pp. 175–223.
Derry, L.A., Keto, L.S., Jacobsen, S.B., Knoll, A.H., Swett, K., 1989. Sr isotopic variations in Upper Proterozoic carbonates from Svalbard and East Greenland. Geochim. Cosmochim. Acta 53 (9), 2331–2339.
Dickin, A.P., 1994. Nd isotope chemistry of Tertiary igneous rocks from Arran, Scotland: implications for magma evolution and crustal structure. Geol. Mag. 131 (3), 329–333.
Duffield, W.A., Ruiz, J., 1998. A model that helps explain Sr-isotope disequilibrium between feldspar phenocryst and melt in large-volume silicic magma system. J. Volcanol. Geoth. Res. 87, 7–13.
Estrada, S., Mende, K., Gerdes, A., Gärtner, A., Hofmann, M., Spiegel, C., Damaske, D., Koglin, N., 2018. Proterozoic to Cretaceous evolution of the western and central Pearya Terrane (Canadian High Arctic). J. Geodyn. 120, 45–76. https://doi.org/10.1016/j.jog.2018.05.010.
Ewart, A., Griffin, W.L., 1994. Application of proton-microprobe data to trace-element partitioning in volcanic-rocks. Chem. Geol. 117 (1–4), 251–284. https://doi.org/10.1016/0009-2541(94)90131-7.
Faehnrich, K., Majka, J., Schneider, D., Mazur, S., Manecki, M., Ziemniak, G., Wala, V.T., Strauss, J.V., 2020. Geochronological constraints on Caledonian strike–slip displacement in Svalbard, with implications for the evolution of the Arctic. Terra Nova 32 (4), 290–299.
Fitton, J.G., Saunders, A.D., Norry, M.J., Hardarson, B.S., Taylor, R.N., 1997. Thermal and chemical structure of the Iceland plume. Earth Planet. Sci. Lett. 153 (3-4), 197–208.
Gayer, R.A., Gee, D.G., Harland, W.B., Miller, J.A., Spall, H.R., Wallis, R.H., Winsnes, T. S., 1966. Radiometric age determinations on the rocks from Spitsbergen. Nor. Polarinst. Skr. 137, 1–39.
Gee, D.G., Teben'kov, A.M., 2004. Svalbard: a fragment of the Laurentian margin. Geological Society, London, Memoirs 30 (1), 191–206.
Gee, D.G., Fossen, H., Henriksen, N., Higgins, A.K., 2008. From the early Paleozoic platforms of Baltica and Laurentia to the Caledonide orogen of Scandinavia and Greenland. Episodes 31 (1), 44–51.
Gee, D.G., Janák, M., Majka, J., Robinson, P., van Roermund, H., 2013. Subduction along and within the Baltoscandian margin during closing of the Iapetus Ocean and Baltica-Laurentia collision. Lithosphere 5, 169–178. https://doi.org/10.1130/L220.1.
Goldstein, S.L., O'Nions, R.K., Hamilton, P.J., 1984. A Sm-Nd isotopic study of atmospheric dusts and particulates from major river systems. Earth Planet. Sci. Lett. 70 (2), 221–236.
Gołuchowska, K., Barker, A.K., Majka, J., Manecki, M., Czerny, J., Bazarnik, J., 2012. Preservation of magmatic signals in metavolcanics from Wedel Jarlsberg Land, SW Svalbard. Mineralogia 43, 179–197.
Gołuchowska, K., Barker, A.K., Czerny, J., Majka, J., Manecki, M., Farajewicz, M., Dwornik, M., 2016. Magma storage of an alkali ultramafic igneous suite from Chamberlindalen, SW Svalbard. Mineral. Petrol. 110, 623–638.
Gumsley, A., Manby, G., Domańska-Siuda, J., Nejbert, K., Michalski, K., 2020. Caught between two continents: first identification of the Ediacaran Central Iapetus Magmatic Province in Western Svalbard with palaeogeographic implications during final Rodinia breakup. Precambr. Res. 341, 105622. https://doi.org/10.1016/j.precamres.2020.105622.
Harland, W.B., 1997. Proto-basement in Svalbard. Polar Res. 16 (2), 123–147.
Henderson, G.M., Martel, D.J., O'Nions, R.K., Shackleton, N.J., 1994. Evolution of sea water $^{87}Sr/^{86}Sr$ over the last 400 ka: the absence of glacial/interglacial cycles. Earth Planet. Sci. Lett. 128, 643–651.
Hjelle, A., 1962. Contribution to the geology of the Heela Hock Formation in Nordenskiöld Land, Vestspitsbergen. Norsk Polarinstitutt Arbok 1961, 83–95.
Hjelle, A., 1967. Stratigraphical correlation of Hecla Hoek successions north and southof Bellsund. Norsk Polarinstitutt Arbok 1967, 46–51.
Hjelle, A., Lauritzen, Ø., Salvigsen, O., Winsnes, T.S., 1986. Geological map of Svalbard 1:100,000. Sheet B10G Van Mijenfjorden. Norsk Polarinstitutt, Oslo 1986.
Hoffman, P.F., Li, Z.-X., 2009. A palaeogeographic context for Neoproterozoic glaciation. Palaeogeogr. Palaeoclimatol. Palaeoecol. 277 (3-4), 158–172.
Hollocher, K., Robinson, P., Walsh, E., Terry, M.P., 2007. The Neoproterozoic Ottfjället dike swarm of the Middle Allochthon, traced geochemically into the Scandian Hinterland, Western Gneiss Region, Norway. Am. J. Sci. 307, 901–953.
Hopf, S., 1993. Behaviour of rare earth elements in geothermal systems of New Zealand. J. Geochem. Explor. 47 (1-3), 333–357.
Jacobsen, S.B., Wasserburg, G.J., 1980. Sm-Nd isotopic evolution of chondrites. Earth Planet. Sci. Lett. 50 (1), 139–155.
Johnson, M.C., Plank, T., 2000. Dehydration and melting experiments constrain the fate of subducted sediments. Geochem. Geophys. Geosyst. 1 (12).
Kośmińska, K., Majka, J., Mazur, S., Krumbholz, M., Klonowska, I., Manecki, M., Czerny, J., Dwornik, M., 2014. Blueschist facies metamorphism in Nordenskiöld Land of west-central Svalbard. Terra Nova 26 (5), 377–386.
Krasil'shchikov, A.A., Kovaleva, G.A., Winsnes, T.S., 1979. Precambrian rock stratigraphic units of the west coast of Spitsbergen. Nor. Polarinst. Skr. 167, 81–88.
Labrousse, L., Elvevold, S., Lepvrier, C., Agard, P., 2008. Structural analysis of high-pressure metamorphic rocks of Svalbard: reconstructing the early stages of the Caledonian orogeny. Tectonics 27 (5).
le Roux, P.J. 2000. The geochemistry of selected mid-ocean ridge basalts from the Southern Mid-Atlantic Ridge (40-55 deg S). Thesis of dissertation, doctoral, University Cape Town, Monography.
le Roux, P., le Roex, A., Schilling, J.-G., 2002a. MORB melting processes beneath the southern Mid-Atlantic Ridge (40–55 S): a role for mantle plume-derived pyroxenite. Contrib. Miner. Petrol. 144 (2), 206–229.
le Roux, P., le Roex, A., Schilling, J.-G., 2002b. Crystallization processes beneath the southern Mid-Atlantic Ridge (40–55 S), evidence for high-pressure initiation of crystallization. Contrib. Miner. Petrol. 142 (5), 582–602.
le Roux, P.J., le Roex, A.P., Schilling, J.-G., Shimizu, N., Perkins, W.W., Pearce, N.J.G., 2002c. Mantle heterogeneity beneath the southern Mid-Atlantic Ridge: trace element evidence for contamination of ambient asthenospheric mantle. Earth Planet. Sci. Lett. 203 (1), 479–498.
MacGeehan, P.J., MacLean, W.H., 1980. An Archean sub-seafloor geothermal system, 'calc-alkali' trends, and massive sulphide genesis. Nature 286, 767–771.
Mahood, G., Hildreth, W., 1983. Large partition coefficients for trace elements in high-silica rhyolites. Geochim. Cosmochim. Acta 47 (1), 11–30. https://doi.org/10.1016/0016-7037(83)90087-X.
Majka, J., Mazur, S., Manecki, M., Czerny, J., Holm, D.K., 2008. Late Neoproterozoic amphibolite-facies metamorphism of a pre-Caledonian basement block in southwest Wedel Jarlsberg Land, Spitsbergen: new evidence from U-Th-Pb dating of monazite. Geol. Mag. 145 (6), 822–830.
Majka, J., Czerny, J., Mazur, S., Holm, D.K., Manecki, M., 2010. Neoproterozoic metamorphic evolution of the Isbjørnhamna Group rocks from south-western Svalbard. Polar Res. 29, 250–264.

Majka, J., Larionov, A.N., Gee, D.G., Czerny, J., Pršek, J., 2012. Neoproterozoic pegmatite from Skoddefjelet, Wedel Jarlsberg Land, Spitsbergen: additional evidence for c. 640 Ma tectonothermal event in the Caledonides of Svalbard. Polish Polar Res. 33, 1–17.
Majka, J., Be'eri-Shlevin, Y., Gee, D.G., Czerny, J., Frei, D., Ladenberger, A., 2014. Torellian (c. 640 Ma) metamorphic overprint of Tonian (c. 950) basement in the Caledonides of southwestern Svalbard. Geol. Mag. 151, 732–748.
Majka, J., Kośmińska, K., Mazur, S., Czerny, J., Piepjohn, K., Dwornik, M., Manecki, M., 2015. Two garnet growth events in polymetamorphic rocks in southwest Spitsbergen, Norway: insight in the history of Neoproterozoic and early Paleozoic metamorphism in the High Arctic. Can. J. Earth Sci. 52 (12), 1045–1061.
Majka, J., Kośmińska, K., 2017. Magmatic and metamorphic events recorded within the Southwestern Basement Province of Svalbard. Arctos 3 (1). https://doi.org/10.1007/s41063-017-0034-7.
Majka, J., Kośmińska, K., Bazarnik, J., McClelland, W.C., 2021. The Ordovician Thores volcanic island arc of the Pearya Terrane from northern Ellesmere Island formed on Precambrian continental crust. Lithos 386-387, 105999. https://doi.org/10.1016/j.lithos.2021.105999.
Manecki, M., Holm, D.K., Czerny, J., Lux, D., 1998. Thermochronological evidence for late Proterozoic (Vendian) cooling in southwest Wedel Jarlsberg Land, Spitsbergen. Geol. Mag. 135 (1), 63–69.
Marschall, H.R., Dorsey Wanless, V., Shimizu, N., Pogge von Strandmann, P.A.E., Elliott, T., Monteleone, B.D., 2017. The boron and lithium isotopic composition of mid-ocean ridge basalts and the mantle. Geochim. Cosmochim. Acta 207, 102–138.
Masters, R.L., Ague, J.J., 2005. Regional-scale fluid flow and element mobility in Barrow's metamorphic zones, Stonehaven, Scotland. Contrib. Mineral. Petrol. 150 (1), 1–18.
Mazur, S., Czerny, J., Majka, J., Manecki, M., Holm, D., Smyrak, A., Wypych, A., 2009. A strike-slip terrane boundary in Wedel Jarlsberg Land, Svalbard, and its bearing on correlations of SW Spitsbergen with the Pearya terrane and Timanide belt. J. Geol. Soc. Lond. 166 (3), 529–544.
McBirney, A.R., 1979. Effects of assimilation. In: Yoder, H.S. (Ed.), The Evolution of the Igneous Rocks' Fiftieth Anniversary Perspectives. Princeton University Press, Princeton, N.J., pp. 307–338
McKenzie, D., O'Nions, R.K., 1991. Partial melt distributions from inversion of rare earth element concentrations. J. Petrol. 32 (5), 1021–1091.
Meyer, R., Nicoll, G.R., Hertogen, J., Troll, V.R., Ellam, R.M., Emeleus, C.H., 2009. Trace element and isotope constraints on crustal anatexis by upwelling mantle melts in the North Atlantic Igneous province: an example from the Isle of Rum, NW Scotland. Geol. Mag. 146 (3), 382–399.
Mottl, M.J., 1983. Metabasalts, axial hot springs, and the structure of hydrothermal systems at mid-ocean ridges. Geol. Soc. Am. Bull. 94 (2), 161. https://doi.org/10.1130/0016-7606(1983)94<161:MAHSAT>2.0.CO;2.
Muecke, G.K., Pride, C., Sarkar, P., 1979. Rare-earth element geochemistry of regional metamorphic rocks. Phys. Chem. Earth 11, 449–464.
Nelson, B.K., Nelson, S.W., Till, A.B., 1993. Nd- and Sr-isotope evidence for Proterozoic and Paleozoic crustal evolution in the Brooks Range, Northern Alaska. J. Geol. 101, 435–450.
Olive, V., Ellam, R., Wilson, L., 2001. A protocol for the determination of the rare earth elements at picomole level in rocks by ICP-MS: results on geological reference material USGS PCC-1 and DTS-1. Geostand. Newsl. 25, 219–228.
Ohta, Y., 1979. Blue schists from Motalafjella, western Spitsbergen. Nor. Polarinst. Skr. 167, 171–217.
Ohta, Y., 1985. Geochemistry of Precambrian igneous rocks between St. Jonsfjorden and Isfjorden, central western Spitsbergen, Svalbard. Polar Res. 3, 49–67.
Pandarinath, K., García-Soto, A.Y., Santoyo, E., Guevara, M., Gonzalez-Partida, E., 2020. Mineralogical and geochemical changes due to hydrothermal alteration of the volcanic rocks at Acoculco geothermal system, Mexico. Geol. J. 55 (9), 6508–6526.
Pearce, J.A., 1976. Statistical analysis of major elements patterns in basalts. J. Petrol. 17, 15–43.
Peate, D.W., Barker, A.K., Rishuus, M.S., Andreasen, R., 2008. Temporal variations in crustal assimilation of magma suites in the East Greenland flood basalt province: Tracking the evolution of magmatic plumbing system. Lithos 102, 179–197.
Pfänder, J.A., Jochum, K.P., Kozakov, I., Kröner, A., Todt, W., 2002. Coupled evolution of back-arc and island arc-like mafic crust in the late-Neoproterozoic Agardagh Tes-Chem ophiolite, Central Asia; evidence for trace elements and Sr-Nd-Pb isotope data. Contrib. Mineral. Petrol. 143, 154–174.
Pin, C., Zalduegui, J.S., 1997. Sequential separation of light rare-earth elements, thorium and uranium by miniaturized extraction chromatography: application to isotopic analyses of silicate rocks. Anal. Chim. Acta 339 (1-2), 79–89.
Plank, T., Langmuir, C.H., 1998. The chemical composition of the subducting sediment and its consequences for the crust and mantle. Chem. Geol. 145, 325–394.
Ridley, W.I., 2012. Petrology of Associated Igneous Rocks. Volcanic massive sulfide occurrence model. U.S. Geological Survey, Reston, Virginia.
Riishuus, M.S., Peate, D.W., Tegner, C., Wilson, J.R., Brooks, C.K., Waight, T.E., 2005. Petrogenesis of syenites at a rifted continental margin: origin, contamination and interaction of alkaline mafic and felsic magmas in the Astrophyllite Bay Complex, East Greenland. Contrib. Mineral. Petrol. 149 (3), 350–371.
Ritzmann, O., Jokat, W., Mjelde, R., Shimamura, H., 2002. Crustal structure between the Knipovich Ridge and the Van Mijenfjorden (Svalbard). Mar. Geophys. Res. 23 (5/6), 379–401.
Ritzmann, O., Jokat, W., Czuba, W., Guterch, A., Mjelde, R., Nishimura, Y., 2004. A deep seismic transect from Hovgård Ridge to northwestern Svalbard across the continental-ocean transition: a sheared margin study. Geophys. J. Int. 157 (2), 683–702.
Roddaz, M., Debat, P., Nikiéma, S., 2007. Geochemistry of Upper Birmian sediments (major and trace elements and Nd-Sr isotope) and implication for weathering and tectonic setting of the Late Paleoproterozoic crust. Precambr. Res. 159, 197–211.
Rudnick, R.L., Gao, S., 2003. The composition of the continental crust. In: Rudnick, R.L. (Ed.), The Crust, Vol. 3. Elsevier-Pergamon, Oxford, pp. 1–64.
Ryan, W.B.F., Carbotte, S.M., Coplan, J.O., O'Hara, S., Melkonian, A., Arko, R., Weissel, R.A., Ferrini, V., Goodwillie, A., Nitsche, F., Bonczkowski, J., Zemsky, R., 2009. Global Multi-Resolution Topography synthesis. Geochem. Geophys. Geosyst. 10 (3), Q03014–/a. https://doi.org/10.1029/2008GC002332.
Schneider, K.P., Kirchenbaur, M., Fonseca, R.O.C., Kasper, H.U., Münker, C., Froitzheim, N., 2016. Role of crustal assimilation and basement compositions in the petrogenesis of differentiated intraplate volcanic rocks: a case study from the Siebengebirge Volcanic Field, Germany. Contrib. Mineral. Petrol. 171 (6) https://doi.org/10.1007/s00410-016-1271-7.
Sellevoll, M.A., Duda, S.J., Guterch, A., Pajchel, J., Perchuc, E., Thyssen, F., 1991. Crustal structure in the Svalbard region from seismic measurements. Tectonophysics 189 (1-4), 55–71.
Skelton, A., Arghe, F., Pitcairn, I., 2010. Regional mapping of pre-metamorphic spilitization and associated chemical mobility in greenschist-facies metabasalts of the SW Scottish Highlands. J. Geol. Soc. 167 (5), 1049–1061.
Skelton, A., Lewerentz, A., Kleine, B., Webster, D., Pitcairn, I., 2015. Structural channelling of metamorphic fluids on Islay, Scotland: implications for paleoclimatic reconstruction. J. Petrol. 56 (11), 2145–2172.
Sobolev, A.V., Migdisov, A.A., Portnyagin, M.V., 1996. Incompatible element partitioning between clinopyroxene and basalt liquid revealed by the study of melt inclusions in minerals from Troodos lavas, Cyprus. Petrology 4 (3), 307–317.
Spera, F.J., Bohrson, W.A., 2001. Energy-Constrained Open-System magmatic processes I: general model and Energy-Constrained Assimilation and Fractional Crystallization (EC-AFC) formulation. J. Petrol. 42, 999–1018.
Sun, S.-s., McDonough, W.F., 1989. Chemical and isotopic systematics of oceanic basalts: implications for mantle composition and processes. Geological Society of London, Special Publications 42 (1), 313–345.
Svenningsen, O.M., 2001. Onset of seafloor spreading in the Iapetus Ocean at 608 Ma: precise age of the Sarek Dyke Swarm, northern Swedish Caledonides. Lithos 110, 241–254.
Taylor, P.N., Kalsbeek, F., Bridgwater, D., 1992. Discrepancies between neodymium, lead and strontium model ages from the Precambrian of southern East Greenland: Evidence for a Proterozoic granulite-facies event affecting Archean gneisses. Chem. Geol. 94, 281–291.
Tegner, C., Andersen, T.B., Kjøll, H.J., Brown, E.L., Hagen-Peter, G., Corfu, F., Planke, S., Torsvik, T.H., 2019. A mantle plume origin for the Scandinavian Dyke Complex: a "piercing point" for 615 Ma plate reconstruction of Baltica? Geochem. Geophys. Geosyst. 20 https://doi.org/10.1029/2018GC007941.
Thompson, R.N., Morrison, M.A., Dickin, A.P., Gibson, I., Harmon, R.S., 1986. Two contrasting styles of interaction between basic magmas and continental crust in the British Tertiary Volcanic Province. J. Geophys. Res. Solid Earth 91 (B6), 5985–5997.
Thorarinsson, S.B., Holm, P.M., Duprat, H., Tegner, C., 2011. Silicic magmatism associated with Late Crateceous rifting in the Arctic Basin – petrogenesis of the Kap Kane sequence, the Kap Washington Group volcanics, North Greenland. Lithos 125, 65–85.
Truong, T.B., Castillo, P.R., Hilton, D.R., Day, J.M.D., 2018. The trace element and Sr-Nd-Pb isotope geochemistry of Juan Fernandez lavas reveal variable contributions from a high $^{3}He/^{4}He$ mantle plume. Chem. Geol. 476, 280–291.
Tütken, T., Eisenhauer, A., Wiegand, B., Hansen, B.T., 2002. Glacial–interglacial cycles in Sr and Nd isotopic composition of Arctic marine sediments triggered by the Svalbard/Barents Sea ice sheet. Mar. Geol. 182 (3-4), 351–372.
Wala, V.T., Ziemniak, G., Majka, J., Faehnrich, K., McClelland, W.C., Meyer, E.E., Manecki, M., Bazarnik, J., Strauss, J.V., 2021. Neoproterozoic stratigraphy of the Southwestern Basement Province, Svalbard (Norway): Constraints on the Proterozoic-Paleozoic evolution of the North Atlantic-Arctic Caledonides. Precambr. Res. 358, 106138. https://doi.org/10.1016/j.precamres.2021.106138.
Winchester, J.A., Floyd, P.A., 1976. Geochemical magma type discrimination application to altered and metamorphosed basic igneous rocks. Earth Planet. Sci. Lett. 28, 459–469.
Zack, T., John, T., 2007. An evaluation of reactive fluid flow and trace element mobility in subducting slabs. Chem. Geol. 239 (3-4), 199–216.
Zhiwei, B., Zhenhua, Z., 2003. Rare-earth element mobility during ore-forming hydrothermal alteration: a case study of Dongping gold deposit Hebei Province, China. Chinese J. Geochem. 22 (1), 45–57.
Ziemniak, G., Kośmińska, K., Schneider, D.A., Majka, J., Lorenz, H., McClelland, W.C., Wala, V.T., and Manecki, M., 2019, Defining tectonic boundaries using detrital zircon signatures of Precambrian metasediments from Svalbard's Southwestern Caledonian Basement Province. In: Piepjohn, K., Strauss, J.V., Reinhardt, L., and McClelland, W.C., (Eds.), Circum-Arctic Structural Events: Tectonic Evolution of the Arctic Margins and Trans-Arctic Links with Adjacent Orogens. Geological Society of America Special Paper 541, Doi: 10.1130/2018.2541(05).